2-1-2008

Interstitials, Vacancies and Dislocations in Flux-Line Lattices: A Theory of Vortex Crystals, Supersolids and Liquids

M. Cristina Marchetti
Syracuse University

Leo Radzihovsky
University of Colorado

Interstitials, Vacancies and Dislocations in Flux-Line Lattices: A Theory of Vortex Crystals, Supersolids and Liquids

M. Cristina Marchetti
Physics Department, Syracuse University, Syracuse, NY 13244

Leo Radzihovsky
Physics Department, University of Colorado, Boulder, CO 80309
(February 1, 2008)

We study a three dimensional Abrikosov vortex lattice in the presence of an equilibrium concentration of vacancy, interstitial and dislocation loops. Vacancies and interstitials renormalize the long-wavelength bulk and tilt elastic moduli. Dislocation loops lead to the vanishing of the long-wavelength shear modulus. The coupling to vacancies and interstitials - which are always present in the liquid state - allows dislocations to relax stresses by climbing out of their glide plane. Surprisingly, this mechanism does not yield any further independent renormalization of the tilt and compressional moduli at long wavelengths. The long wavelength properties of the resulting state are formally identical to that of the "flux-line hexatic" that is a candidate "normal" hexatically ordered vortex liquid state.

I. INTRODUCTION

Both disorder and thermal fluctuations strongly affect the properties of the vortex array induced in type II superconductors by an external magnetic field.[1–3]. One of the most striking consequences of thermal fluctuations, particularly pronounced in the high-T_c materials, is the resistive vortex liquid state,[4] located between the $H_{c2}(T)$ line and the vortex solid in the magnetic field (H)-temperature (T) phase diagram.[5] Upon field cooling, a vortex liquid freezes into an Abrikosov vortex solid. The nature of the freezing transition and of the resulting vortex solid phase depends on the amount of disorder present in the material. In dirty samples the vortex solid has been described as a "vortex glass",[6] and its translational correlation length is limited by disorder to a *finite* value.[7] In three dimensions, the low temperature vortex glass solid is expected to be a true superconductor with a vanishing *linear* resistivity. For weak disorder, the vortex solid state is expected to be a topologically ordered "Bragg" glass state in three dimensions, with logarithmically growing vortex displacements, but bound dislocation loops.[8] The freezing transition of the vortex array has been observed to be first order[9,11] in ultra clean samples and continuous in dirty superconductors.[9–13]

In very clean samples, where the disorder-limited translational correlation length is thousands of intervortex lattice constants, the low temperature phase can be well approximated by a vortex *lattice*. Within an elastic description, the primary low temperature excitations of the vortex lattice are phonons, characterizing two-dimensional displacements of vortex lines from their preferred lattice positions. As the temperature (or field) is raised towards the melting transition, other excitations become important. By definition, these are *defects* in the vortex lattice, i.e. they are not describable in terms of single-valued vortex displacements. These line defects are dislocations, disclinations, vacancies and interstitials and must be included in the model for a complete description of the melting of the vortex solid and of the properties of the resulting vortex liquid state.

At low temperatures, in a well-ordered Abrikosov lattice state,[8] these defects are bound, as the energy of an isolated *line* defect diverges with system size. At higher temperatures entropy can, however, drive a proliferation of these line defects, in analogy with the melting of two-dimensional solids.[14,15] Two melting scenarios are possible:[12] (i) a one-stage first order transition from a solid to an *isotropic* vortex liquid where *both* dislocations and disclinations unbind simultaneously (as it occurs in the melting of ordinary 3d solids), (ii) a two-stage, possibly continuous transition[13], where dislocations unbind first, leading to a hexatic flux-line liquid with residual bond-orientational order, vanishing shear modulus, but finite hexatic stiffness. This first transition would then be followed by a proliferation of disclination loops, thereby completing the transition into an *isotropic* vortex liquid. The first stage of this second scenario for the melting of the Abrikosov lattice was first suggested by Marchetti and Nelson.[16] While avoiding the subtle question of the melting transition itself, they adapted the method developed long ago by Nelson and Toner[17] to describe the vortex line-liquid state. Marchetti and Nelson described the hexatic vortex liquid as a vortex lattice with an equilibrium concentration of dislocation loops, treating the latter in the Debye-Huckle approximation. Through detailed calculations, they demonstrated that dislocations drive the long wavelength shear modulus of the system to zero and computed the effective hexatic stiffness of the resulting orientationally ordered vortex liquid.[16]

Vacancies and interstitials constitute another class of defects that play an important role in solids. In ordinary

crystals and in 2d vortex lattices, these *point* defects cost finite energy and are therefore present in finite density, at *any finite* temperature. While their static effects in these systems are minimal, their density represents an important hydrodynamic mode which must be included in the correct description of crystal hydrodynamics.[18]

In strong contrast, in vortex lattices, vacancies and interstitials are *line* defects with energy proportional to their length and thereby diverging in bulk samples. Hence one expects that at low temperatures their average density vanishes. At higher temperatures, this positive energetic contribution to the free energy can, however, be compensated by a negative entropic contribution associated with line wandering, which also scales with the defect length, in analogy with the Kosterlitz-Thouless picture.[14] These considerations allow two thermodynamically distinct crystalline phases, with a sharp phase transition between them. While in both phases dislocations and disclinations are bound, and as a consequence there is long-range translational order (true Bragg spots in an X-ray scattering experiment) and a finite shear modulus, line vacancies and interstitials are bound in the low temperature crystal, but have proliferated in the high temperature crystal phase. A thermodynamically sharp distinction between these two crystal phases in three-dimensional vortex systems was first emphasized by M.P.A. Fisher and Lee[19] based on the mathematical correspondence between vortex lines and world-lines of two-dimensional quantum bosons. In this mapping the low temperature vortex crystal maps onto a 2d Wigner crystal and the high temperature vortex solid corresponds to the quantum supersolid phase of 2d bosons, with vacancies and interstitials in its ground state. The quantum supersolid is quite exotic, in that it is both crystalline and superfluid. Correspondingly, due to the finite density of vacancies and interstitials in the vortex supersolid, vortex lines can move arbitrarily far and entangle, as in a vortex liquid, and therefore this phase exhibits finite linear resistivity.

While experiments seem to rule out the existence of an equilibrated vortex supersolid phase in bulk 2d *quantum* crystals, based on detailed calculations, Frey, Nelson and D.S. Fisher,[20] have argued that such a phase is more likely to exist in flux-line arrays at high fields because of the layered structure of high temperature superconductors. These authors conclude that a vortex supersolid phase will certainly exist in anisotropic superconductors for magnetic fields above a decoupling field B_x where vortices in different CuO_2 layers are essentially decoupled by thermal fluctuations.[21] Furthermore, even if an equilibrium supersolid phase was absent, an appreciable nonequilibrium density of vacancies and interstitials may still be present in a flux-line lattice, when the vortex array undergoes a first order freezing transition upon cooling in a constant field.

In this paper we study the effects of vacancies and interstitials within the vortex supersolid and liquid phases. As discussed above, in the supersolid phase, aside from being responsible for its existence, these defects provide a mechanism for vortex line wandering and consequently for its finite resistivity. They also are important degrees of freedom, in addition to phonons, that must be incorporated in the correct description of the supersolid. In Sec.III we construct a model of a vortex supersolid, as an elastic lattice with an equilibrium concentration of unbound vacancies and interstitials. We compute the flux-line density correlation functions, that characterize the static equilibrium properties of this phase, and extract from these the effective elastic moduli of the supersolid phase. We find that the long-wavelength shear modulus is unaffected by the *fluctuations* in the density of vacancies and interstitials. This result is consistent with the vacancy-interstitials' inability to relax shear, and confirms the finiteness of the supersolid shear rigidity which distinguishes it from a vortex liquid. We also compute a finite, downward renormalization of the compressional and tilt moduli by vacancy and interstitial density fluctuations. We demonstrate that as a consequence of the reduction of the effective tilt modulus, the flux-line *wandering* is enhanced and, analogously to a vortex liquid, a bulk vortex supersolid is always entangled, i.e., it does not exhibit longitudinal superconductivity.

The existence of a vortex supersolid allows for two scenarios for the melting transition into the vortex liquid state. At low magnetic fields, we expect[20] this transition to be directly from the low temperature, non-supersolid crystal into a vortex liquid phase. As discussed above, the vortex liquid state itself can be either a fully disordered isotropic liquid or a bond-orientationally ordered liquid that can further disorder into an isotropic liquid via disclination unbinding.

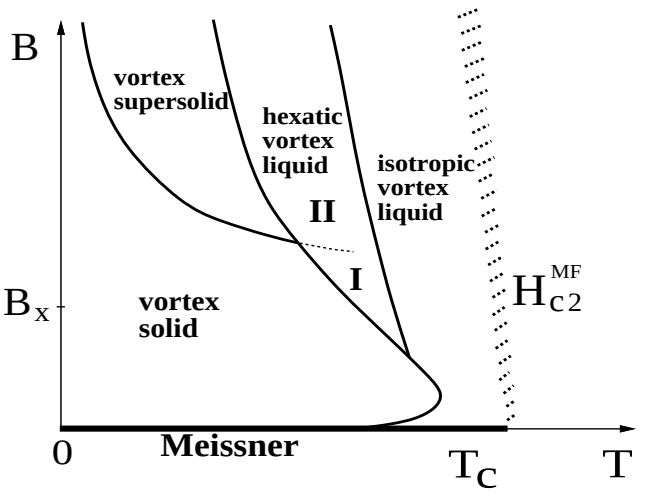

Fig.1.Schematic $B-T$ phase diagram illustrating the flux line crystal, vortex "supersolid" (guaranteed to exist at fields much higher than the decoupling field B_x), the orientationally ordered hexatic vortex liquid, and the isotropic vortex liquid.

Alternatively, the non-supersolid crystal can first undergo a transition into a vortex supersolid by a prolif-

eration of vacancies and interstitials,[20] and subsequently melt into a vortex liquid.[22] These two scenarios have been dubbed as type I and type II melting, respectively,[20] and are illustrated in Fig.1.

Very recent experiments investigating vortex penetration through surface barriers in the presence of a transport current in clean BSCCO samples have indeed indicated that the nature of the melting line may change at high field, even in the absence of point disorder.[23] In fact these experiments suggest the existence of an intermediate phase between the solid and the liquid at high fields. This observed regime lies above the first order melting line determined by equilibrium magnetization measurements, but apparently exhibits a certain amount of sixfold periodicity, as indicated by neutron scattering.[24] It is therefore a candidate for either the supersolid or the hexatic liquid phases studied here.

Although the nature of the type I and type II melting transitions should be quite different,[25] in either case vacancies and interstitials should proliferate in the resulting vortex liquid state.[26] Hence, in addition to dislocations, vacancy and interstitial defects *must* be taken into account for the proper description of a vortex liquid. They were not, however, explicitly included in the calculations of Ref. 16. When vacancies and interstitials are absent, dislocation loops in the vortex line-lattice are restricted to lie in the plane defined by the magnetic field axis and their Burger's vector, and can only glide (see Fig.5), but not climb. One of the consequences of this is that the effective tilt modulus of the vortex liquid is not renormalized by dislocations and in the model of Ref. 16 is therefore identical to that of the vortex lattice.

The results presented in Sec.IV remedy the limitations of Ref. 16, by explicitly including vacancies and interstitials in the description of a vortex liquid. Vacancies and interstitials renormalize the tilt and compressional moduli and allow dislocation loops to climb out of their glide plane by absorbing and emitting these defects. At long wavelengths, however, the coupling of dislocations to vacancies and interstitials does not yield any *additional independent* renormalization of the tilt and compressional moduli. Whether this is a general property of the vortex lattice, or an artifact of the quadratic model and the Debye-Huckel approximation used here, remains an open question. Our work yields a complete description of a bond-orientationally ordered hexatic vortex liquid, whose tilt and bulk moduli are renormalized by dislocations, vacancies and interstitials, and whose shear modulus is driven to zero by the proliferation of these defects.

Our results characterizing the properties of the various phases shown in Fig.1 are summarized in the two tables below. We stress that hexatic I and hexatic II are not two distinct hexatic phases, but rather two different regimes within the same hexatic phase, distinguished by a high and low concentration of vacancy/interstitial defects, respectively. The crossover between these two regimes is indicated in Fig.1 by a dotted line. The results quoted in Table 1 for the hexatic I phase are those obtained by Marchetti and Nelson in Ref. 16 assuming that no vacancy/interstitial defects are present in the system. These results, however, only apply well below the dotted line in Fig.1, very close to the solid-hexatic phase boundary. As the transition to the isotropic liquid is approached, the large number of interacting dislocation loops present in the hexatic will invitably generate vacancy/interstitial defects as well, leading to the breakdown of the model of Ref. 16. The type of long-range order present or absent in each of these phases is summarized qualitatively in Table 2.

	shear	compression	tilt	$\langle W^2 \rangle$ (Eq. (3.28))
crystal	c_{66}	c_{11}	c_{44}	0
supersolid	c_{66}	$\frac{c_{11}\chi^{-1}-\gamma^2}{c_{11}+\chi^{-1}+2\gamma}$	$\frac{c_{44}K-\gamma'^2}{c_{44}+K+2\gamma'}$	$\frac{n_0^2 k_B T}{K}$
hex II	0	$c_{11}-c_{66}$	$\frac{c_{44}K-\gamma'^2}{c_{44}+K+2\gamma'}$	$\frac{n_0^2 k_B T}{c_{44}}\left[1+\frac{(c_{44}-\gamma')^2}{c_{44}K-\gamma'^2}\right]$
hex I	0	$c_{11}-c_{66}$	c_{44}	$\frac{n_0^2 k_B T}{c_{44}}$

Table 1. A summary of our results for the elastic constants and the winding number in the various phases of Fig. 1.

	Translational LRO	Orientational LRO	Longitudinal Superconductivity
crystal	yes	yes	yes
supersolid	yes	yes	no*
hex I	no	yes	no
hex II	no	yes	no
liquid	no	no	no

Table 2. This table displays the presence or absence of translational and orientational long-range order (LRO) as well as longitudinal superconductivity in each phase. The asterisk serves to emphasize that although the supersolid does not exhibit longitudinal superconductivity, the degree of screening of longitudinal currents in this phase is substantially different from that of the vortex liquid phase (see Table 1).

II. ELASTIC PROPERTIES OF DEFECT-FREE VORTEX LATTICES

A. Model

We begin by recalling the properties of an ordered, *defect-free* vortex lattice, which we expect to be stable at low temperature and field in a clean superconductor.[8] As discussed in the Introduction, long-scale degrees of freedom of this system are uniquely characterized by a single-valued vortex displacement field, $\mathbf{u}(\mathbf{r})$. With the convection in which the external magnetic field $\mathbf{H}_0$ (aligned with the c axis of the superconductor) points along the z axis, the two-dimensional vector displacement $\mathbf{u}(\mathbf{r}_\perp, z)$ is confined to the xy plane.

The long-wavelength properties of a triangular flux-line lattice are characterized by the elastic free energy functional

$$F_{\rm latt} = \frac{1}{2}\int d\mathbf{r}\Big[2c_{66}u_{ij}^2 + (c_{11}-2c_{66})u_{kk}^2 + c_{44}(\partial_z \mathbf{u})^2\Big], \tag{2.1}$$

where

$$u_{ij} = \frac{1}{2}(w_{ij}+w_{ji}) \tag{2.2}$$

is the symmetrized two-dimensional strain tensor, with

$$w_{\alpha j} = \partial_\alpha u_j, \tag{2.3}$$

a 3×2 hybrid strain tensor. Greek indices take on the full three-dimensional set of labels x, y, z, and Latin indices are reserved for the purely two-dimensional set x, y. We will use this notation throughout the manuscript. The parameters c_{66}, c_{11} and c_{44} appearing in the Eq.2.1 are the shear, compressional and tilt modulus, respectively.[27] In contrast to ordinary crystals, in a flux-line lattice vortex interactions extend over a range of order of the London penetration depth, λ, which can be quite large, especially in high T_c superconductors. As emphasized in the extensive literature on the subject,[28,2] on scales shorter than λ, this leads to wavevector-dependent elastic moduli. For a detailed comparison with experiments, inclusion of these nonlocal elastic effects can be important, especially at high fields, and they can be easily incorporated into our results by replacing all of the *bare* elastic moduli by the proper wavevector-dependent expressions.[29]

When the lattice contains no vacancies nor interstitials, the number of flux lines equals the number N of sites in the triangular lattice. On the average, the flux lines are aligned with the external field and the equilibrium magnetic flux density field is given by $\mathbf{B}_0 = \hat{\mathbf{z}}B_0 = \hat{\mathbf{z}}\phi_0 n_0$, where $\phi_0 = hc/2e$ is the flux quantum, $n_0 = N/A \equiv 1/a_c$ is the equilibrium number density of vortex lines and a_c the area of the primitive unit cell.

Fluctuations in the local induction $\delta\mathbf{B}(\mathbf{r}) = \mathbf{B}(\mathbf{r}) - \mathbf{B}_0$ can be described in terms of fluctuations in the areal density of flux lines, $\delta n(\mathbf{r}_\perp, z) = n(\mathbf{r}_\perp, z) - n_0$, and of a tilt vector field $\mathbf{t}(\mathbf{r}_\perp, z)$, with the relation

$$\delta B_z = \phi_0 \delta n, \tag{2.4}$$

$$\mathbf{B}_\perp = \phi_0 \mathbf{t}, \tag{2.5}$$

valid in the long wavelength $q\lambda << 1$ limit.[31] In the absence of vacancies and interstitials, the areal density of flux lines and their orientation relative to the applied field direction are entirely determined by the local strains, according to

$$\delta n/n_0 = -\delta A/A = -u_{ii}, \tag{2.6}$$

$$\mathbf{t}/n_0 = \partial_z \mathbf{u}. \tag{2.7}$$

The condition $\boldsymbol{\nabla}\cdot\mathbf{B} = 0$ translates into a "continuity" constraint for the flux lines,

$$\partial_z \delta n + \boldsymbol{\nabla}_\perp \cdot \mathbf{t} = 0. \tag{2.8}$$

As can be seen from Eqs.2.6 and 2.7, this continuity constraint is identically satisfied in the *defect-free* vortex lattice, where the displacement $\mathbf{u}$ is single-valued.

B. Correlation and response functions

Thermal fluctuations in the density and tilt field are characterized by the density-density correlation function (the structure factor),

$$S(q_\perp, q_z) = \frac{1}{V}\langle \delta n(\mathbf{q}) \delta n(-\mathbf{q})\rangle, \tag{2.9}$$

and the tilt field correlation function,

$$\begin{aligned} T_{ij}(q_\perp, q_z) &= \frac{1}{V}\langle t_i(\mathbf{q}) t_j(-\mathbf{q})\rangle \\ &= T_L(q_\perp, q_z) P^L_{ij}(\hat{\mathbf{q}}_\perp) + T_T(q_\perp, q_z) P^T_{ij}(\hat{\mathbf{q}}_\perp), \end{aligned} \tag{2.10}$$

where

$$P^L_{ij}(\hat{\mathbf{q}}_\perp) = \hat{q}_{\perp i}\hat{q}_{\perp j}\ , \tag{2.11}$$

$$P^T_{ij}(\hat{\mathbf{q}}_\perp) = \delta_{ij} - \hat{q}_{\perp i}\hat{q}_{\perp j}\ , \tag{2.12}$$

are the longitudinal and the transverse projection operators, respectively, $\hat{\mathbf{q}}_\perp = \mathbf{q}_\perp/q_\perp$, and V is the volume of the superconductor. In light of the constraint, Eq.2.8, the longitudinal part of the tangent field correlator is proportional to the structure function, with

$$T_L(q_\perp, q_z) = \frac{q_z^2}{q_\perp^2} S(q_\perp, q_z). \tag{2.13}$$

The brackets $\langle \ldots \rangle$ in above expressions and throughout the paper indicate a thermal average with a Boltzmann weight $e^{-F/k_BT}/Z$, with F the free energy functional and $Z = \mathrm{Trace}[e^{-F/k_BT}]$ the corresponding partition function. In the defect-free (non-supersolid) vortex lattice, F is given by $F_{\rm latt}$, Eq.2.1, and we denote the corresponding thermal averages by $\langle \ldots \rangle_0$. Using Eqs.2.6 and 2.7, the structure function and the tilt field correlation function can be expressed in terms of thermal averages of the phonon field $\mathbf{u}$, and are therefore easily computed, with the result,

$$\begin{aligned} S^0(\mathbf{q}) &= \frac{q_\perp^2 n_0^2}{V}\langle |\hat{\mathbf{q}}_\perp \cdot \mathbf{u}(\mathbf{q})|^2\rangle_0 \\ &= \frac{n_0^2 k_B T q_\perp^2}{c_{11} q_\perp^2 + c_{44} q_z^2}, \end{aligned} \tag{2.14}$$

and

$$\begin{aligned} T^0_T(\mathbf{q}) &= \frac{q_z^2 n_0^2}{V} P^T_{ij}(\hat{\mathbf{q}}_\perp)\langle u_i(\mathbf{q}) u_j(-\mathbf{q})\rangle_0 \\ &= \frac{n_0^2 k_B T q_z^2}{c_{66} q_\perp^2 + c_{44} q_z^2}. \end{aligned} \tag{2.15}$$

The structure function $S(\mathbf{q})$ can be probed in a neutron scattering experiment. The tilt correlation function $T_{ij}(\mathbf{q})$ is directly connected to the experimentally measurable linear magnetic susceptibility tensor, $\chi_{ij}(\mathbf{q})$, according to

$$4\pi\chi_{ij}(q_\perp, q_z) = -\delta_{ij} + \frac{\phi_0^2}{4\pi k_B T} T_{ij}(q_\perp, q_z). \tag{2.16}$$

Equation 2.16 holds in the long wavelength $q\lambda << 1$ limit. A more general relationship between susceptibility and tilt correlation function that applies at scales shorter than λ in an anisotropic material can be found for instance in Ref. 35. The first term on the right hand side of Eq.2.16 represents a perfect diamagnetic (negative) Meissner response, which, in a mixed state is considerably reduced by the "normal" paramagnetic vortex tilt response T_{ij}, contained in the second term. The linear susceptibility relates the transverse flux density $\delta\mathbf{B}_\perp(\mathbf{q})$ induced by an external perturbation field $\delta\mathbf{H}_\perp(\mathbf{q})$, applied perpendicular to the field $\mathbf{H}_0 = \hat{\mathbf{z}}H_0$ responsible for the onset of the vortex state, with

$$\delta B_{\perp i}(\mathbf{q}) = [\delta_{ij} + 4\pi\chi_{ij}(\mathbf{q})]\delta H_{\perp j}(\mathbf{q})\ . \tag{2.17}$$

From Eq.2.15, appropriate for a perfect, defect-free flux-line lattice, we observe that the long wavelength limit of the transverse part of the tilt field correlation function is *nonanalytic*, with

$$T^0_T(q_\perp = 0, q_z) = \frac{n_0^2 k_B T}{c_{44}}\ , \tag{2.18}$$

$$T^0_T(q_\perp, q_z = 0) = 0\ . \tag{2.19}$$

The nonanalyticity of the tilt correlation function reflects a drastically different linear response of the defect-free vortex lattice to two types of transverse field perturbations.[32]

The transverse field response in the limit $q_\perp << q_z \to 0$, corresponds to a tilt perturbation of the flux lines, induced by an applied transverse field $V\delta_{\mathbf{q}_\perp,\mathbf{0}}\delta\mathbf{H}_\perp(q_z)$ that is spatially homogeneous in the xy plane. The corresponding long wavelength transverse susceptibility, $\chi_T = P^T_{ij}\chi_{ij}$, is given by

$$\lim_{q_z\to 0}\chi^0_T(q_\perp = 0, q_z) = -\frac{1}{4\pi}\Big[1 - \frac{B^2}{4\pi c_{44}}\Big]. \tag{2.20}$$

If the second term in brackets on the right hand side of Eq.2.20 were absent, the superconductor would exhibit perfect screening of the transverse perturbation. Such a behavior can for instance occur in flux-line arrays pinned by aligned damage tracks. In the presence of such correlated disorder, the vortex lattice is replaced by a thermodynamically distinct "Bose" glass phase,[33] that is characterized by a divergent tilt modulus c_{44} and exhibits a transverse Meissner effect, with $\lim_{q_z\to 0}\chi_T(q_z) = -1/4\pi$. In the absence of *anisotropic* pinning of the vortex lattice, such a perfect transverse diamagnetic response is spoiled by the finite vortex tilt response, that leads to only a partial screening of the transverse field, displayed in Eq.2.20.

Conversely, the limit $q_z << q_\perp \to 0$, describes a magnetic response to a transverse field $V\delta_{q_z,0}\delta\mathbf{H}_\perp(\mathbf{q}_\perp)$ that is homogeneous along the z-axis, but is spatially varying in the xy-plane. The induced z-directed screening currents lead to a shear perturbation of the flux-line array, with the response in a defect-free lattice given by

$$\lim_{q_\perp\to 0}\chi^0_T(q_\perp, q_z = 0) = -\frac{1}{4\pi}. \tag{2.21}$$

Thus the flux lattice exhibits perfect screening in response to this z-independent transverse perturbation. Since the screening currents involved in the shear perturbation run parallel to the applied field $\mathbf{H}_0 \parallel \hat{\mathbf{z}}$, a perfect Meissner response to a shear perturbation has also been termed longitudinal superconductivity. It follows directly from the fact that, in contrast to a liquid, a vortex lattice is characterized by a finite shear modulus c_{66}.

For comparison, we recall that in a flux-line liquid, the long wavelength limit of the transverse part of the tilt correlation function is analytic, with

$$\lim_{q_\perp \to 0} T_T^{\rm liquid}(q_\perp, q_z = 0) = \lim_{q_z \to 0} T_T^{\rm liquid}(q_\perp = 0, q_z) \ , \\ = \frac{n_0^2 k_B T}{c_{44}^{\rm liquid}} \ . \qquad (2.22)$$

As expected, a vortex liquid, being *qualitatively* identical to the normal state, albeit highly conductive, exhibits neither transverse Meissner effect, nor longitudinal superconductivity. We will return to this point again in Sec.IV.

Finally, we note that in the latter $q_z << q_\perp \to 0$ limit, the transverse part of the tilt correlation function corresponds to the world-lines winding number $\langle W^2 \rangle$ studied by Pollock and Ceperley[34] in their path integral approach to the superfluid transition in quantum boson systems. In such an approach, dating back to Feynman, the superfluid phase is identified with an entangled state of boson world-line trajectories,

$$\lim_{q_\perp \to 0} T_T(q_\perp, q_z = 0) = \langle W^2 \rangle \ , \qquad (2.23)$$

$$= \frac{\hbar n_s}{m} \ , \qquad (2.24)$$

and n_s the boson superfluid density. The well-known identification of physical parameters under the boson–vortex mapping is given by

$$\hbar \leftrightarrow k_B T \ , \qquad (2.25)$$

$$m \leftrightarrow \tilde{\epsilon}_1 \ , \qquad (2.26)$$

$$\hbar\beta \leftrightarrow L \ , \qquad (2.27)$$

with m the boson mass, $\tilde{\epsilon}_1$ the core energy per unit of length of a single vortex line, β the inverse boson temperature and L the vortex sample thickness. Utilizing this mapping, together with the approximate local expression for the tilt modulus $c_{44} = n_0 \tilde{\epsilon}_1$, we reassuringly find that the defect-free flux-line lattice (in which vortex lines do not entangle and the sample exhibits longitudinal superconductivity) corresponds to the "normal" boson crystal with vanishing superfluid density $n_s = 0$. The entangled flux-line liquid, on the other hand, corresponds to the superfluid phase of bosons with $n_s = n_0$, and does not exhibit longitudinal superconductivity. We stress, however, that the mapping described above, as well as Eqs. 2.23 and 2.24, only apply to a model of the vortices that neglects the nonlocality of the intervortex interaction along the field (z) direction.[35] A more general approach to the derivation of vortex liquid hydrodynamics, directly from a "kinetic theory" of interacting flux lines was developed in Ref. 36.

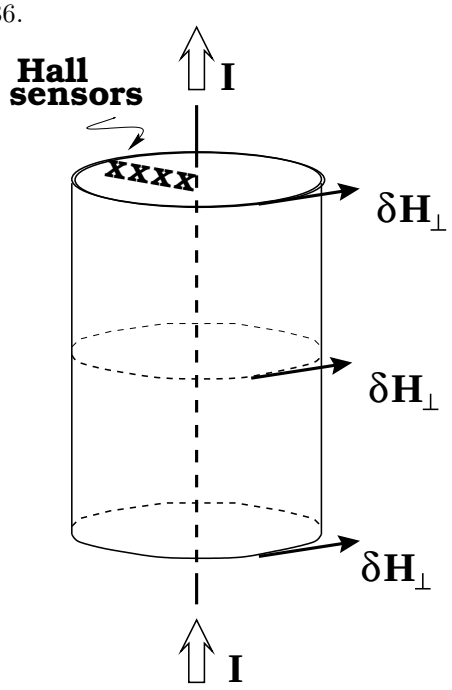

Fig.2.Sketch of an idealized experimental setup to probe longitudinal superconductivity.

Figure 2 shows a sketch of an idealized experimental setup that could be used to probe longitudinal superconductivity. An external field $\mathbf{H}_0$ is applied along the axis (z in our coordinate system) of a cylindrical sample and a uniform vortex state with flux lines running along z is set up. A current I confined to a wire running along the axis of the cylinder and producing an additional azimuthal magnetic field $\delta\mathbf{H}_\perp(\mathbf{r}_\perp) = 2I\hat{\mathbf{z}} \times \mathbf{r}_\perp/(r_\perp^2 c)$, which provides the shear perturbation described above, can therefore probe the $q_z = 0$ field response of the vortex state. The longitudinal superconductivity can then be studied by measuring the induced azimuthal component $B_\phi(r_\perp)$ of the local induction inside the sample. This may be possible by placing radially-directed row of Hall sensors at the top of the sample. In the defect-free crystal, which is a longitudinal superconductor, we expect $B_\phi = 0$ everywhere in the bulk of the sample, deeper than the penetration length λ from the surface of the cylinder. In contrast in the supersolid and hexatic phases there will be a nonvanishing azimuthal response $B_\phi(r_\perp)$ everywhere in the sample.

III. ELASTIC PROPERTIES OF SUPERSOLIDS

A. Model

As discussed in the Introduction, we expect that upon increasing the temperature and the external magnetic field, the defect-free vortex crystal will undergo a thermodynamically sharp transition into a vortex supersolid, characterized by the coexistence of crystalline order and a finite equilibrium density of vacancy and interstitial defects.[20] Our goal here is to develop a continuum description of the long wavelength elastic properties of such a supersolid phase.

Once vacancy and interstitial line defects proliferate in the supersolid, their positions and orientations represent new and important low-energy degrees of freedom, independent of the lattice displacements characterized by the field $\mathbf{u}(\mathbf{r})$. At finite temperature, these defects will lead to fluctuations in the local induction, independent, but energetically coupled to, local elastic strains. To incorporate such defect fluctuations, we adapt the hydrodynamic methods developed for vortex lines,[37,36] to the hydrodynamics of the vacancy and interstitial line-liquid.

At finite density, i.e., within the vortex supersolid phase, the low-energy vacancy and interstitial configurations can be parameterized by *z-directed* conformations $(\mathbf{r}_n^a(z), z)$, (with $a = i, v$ denoting interstitial and vacancy, respectively) as they traverse the sample along the direction of the applied field, in close analogy to vortex lines themselves. Long wavelength properties of a gas of N_v vacancies and N_i interstitials can then be described in terms of a net areal density of defects,

$$n_d(\mathbf{r}_\perp, z) = n_i(\mathbf{r}_\perp, z) - n_v(\mathbf{r}_\perp, z) \ , \tag{3.1}$$

and a two-dimensional tilt vector field,

$$\mathbf{t}_d(\mathbf{r}_\perp, z) = \mathbf{t}_i(\mathbf{r}_\perp, z) - \mathbf{t}_v(\mathbf{r}_\perp, z) \ , \tag{3.2}$$

where

$$n_a(\mathbf{r}_\perp, z) = \sum_{n=1}^{N_a} \delta^{(2)}(\mathbf{r}_\perp - \mathbf{r}_n^a(z)) \ , \tag{3.3}$$

and

$$\mathbf{t}_a(\mathbf{r}_\perp, z) = \sum_{n=1}^{N_a} \frac{\partial \mathbf{r}_n^a(z)}{\partial z} \delta^{(2)}(\mathbf{r}_\perp - r_n^a(z)) \ . \tag{3.4}$$

Here $n_d(\mathbf{r}_\perp, z)$ represents the net number of defect lines crossing a unit area perpendicular to the field direction, while $t_{di}(\mathbf{r}_\perp, z)$ is the net number of defect lines crossing a unit area normal to the i-th direction, with $i = x, y$. Since the interaction among vacancy and interstitial defects is short-ranged, we expect that a liquid of such defects be characterized by a compressibility (inverse defect bulk modulus), χ, and a finite tilt modulus, K. The corresponding long-wavelength free energy functional is therefore given by

$$F_d = \frac{1}{2n_0^2} \int d\mathbf{r} \Big[\chi^{-1} (\delta n_d)^2 + K (\mathbf{t}_d)^2 \Big] \ , \tag{3.5}$$

with $\delta n_d = n_d - n_d^0$, and n_d^0 the mean net defect density in equilibrium.

In the presence of these defects, fluctuations in the local magnetic induction (or in the corresponding *flux*-line density $n(\mathbf{r})$ and *flux* tangent field $\mathbf{t}(\mathbf{r})$) can be brought about by changes in both the local lattice strains $w_{\alpha j}$ and the defect densities n_d and $\mathbf{t}_d$, as

$$\delta n = -n_0 w_{ii} + \delta n_d \ , \tag{3.6}$$

and

$$t_i = n_0 w_{zi} + t_{di} \ . \tag{3.7}$$

In this case the continuity equation (2.8), arising from $\boldsymbol{\nabla} \cdot \mathbf{B} = 0$ yields the *nontrivial* constraint

$$\partial_z \delta n_d + \boldsymbol{\nabla}_\perp \cdot \mathbf{t}_d = 0 \ , \tag{3.8}$$

that defect lines cannot start nor stop inside the sample. The *elastic* strain drops out from Eq.3.8, as it identically satisfies the constraint due to the single-valuedness of the displacement field $\mathbf{u}(\mathbf{r})$.

Since motion of defects microscopically corresponds to hopping of vortex lines, we expect an energetic coupling between fluctuations in the density and orientation of defects and the elastic strain field. The lowest order coupling allowed by symmetry corresponds to the following interaction part of the free energy functional

$$F_{int} = \frac{1}{n_0} \int d\mathbf{r} \Big[\gamma \delta n_d \boldsymbol{\nabla} \cdot \mathbf{u} + \gamma' \mathbf{t}_d \cdot \partial_z \mathbf{u} \Big] \ , \tag{3.9}$$

where γ and γ' are positive phenomenological coupling constants with dimensions of elastic moduli. Ignoring a weak coupling to fluctuations in the local temperature, the free energy functionals F_{int} and F_d, together with the elastic part $F_{\rm latt}$, Eq.2.1, completely determine the long-scale elastic properties of the vortex supersolid.

It is important to note that the parameters $c_{11}, c_{66}, c_{44}, \gamma, \gamma', \chi$, and K, appearing in our model, are functions of the *mean* net defect density n_d^0,[38] which, within the supersolid phase, can in principle be determined through detailed microscopic calculations of the type presented in Ref. 20. At the vortex-crystal to supersolid transition, we expect these parameters to display a nonanalytic behavior as a function of the distance from the transition, $|T - T_{xss}|$ (where T_{xss} denotes the crystal-to-supersolid transition temperature), of the form illustrated for $c_{66}(n_d^0(T))$ in Fig.3.

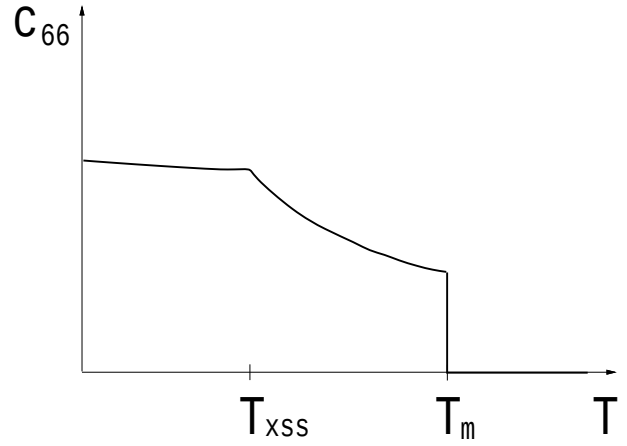

Fig.3. A sketch illustrating the behavior of the elastic shear modulus c_{66} near the vortex crystal to vortex supersolid transition. The proliferation of vacancies and interstitials is responsible for the softening of the effective shear modulus inside the supersolid phase.

In addition to these mean-field effects, the coupling of the elastic degrees of freedom to the *fluctuations* in defect density (around the average n_d^0) and orientation field, Eq.3.9, yields further renormalization of the elastic constants, study of which is in part the focus of our work here.

B. Correlation and response functions

The elastic properties of supersolids can be characterized in a number of distinct ways, reflecting a variety of experimental probes that couple differently to the supersolid degrees of freedom. The simplest of these, from the theoretical and experimental points of view, is the extension of the equal-time equilibrium correlation functions $S(\mathbf{q})$ and $T_{ij}(\mathbf{q})$ defined by Eqs.2.9 and 2.10, respectively. They directly measure fluctuations in the local magnetic induction $\mathbf{B}(\mathbf{r})$, related to the fluctuations in the *total* vortex-line number and tilt densities, via relations (2.4) and (2.5). These latter quantities are determined by *both* the local elastic strain and the defect density fields through Eqs.3.6 and 3.7, and lead to

$$S^{ss}(\mathbf{q}) = \frac{1}{V}\langle |n_0 w_{ii}(\mathbf{q}) - \delta n_d(\mathbf{q})|^2\rangle \ , \tag{3.10}$$

$$T^{ss}_{ij}(\mathbf{q}) = \frac{1}{V}\langle (n_0 w_{zi}(\mathbf{q}) + t_{di}(\mathbf{q}))(n_0 w_{zj}(-\mathbf{q}) + t_{dj}(-\mathbf{q}))\rangle \ . \tag{3.11}$$

In the above, the brackets denote a thermal average evaluated with the total *supersolid* free energy functional which includes both the elastic and the defects degrees of freedom, given by

$$F_{ss} = F_{\rm latt} + F_d + F_{int} \ . \tag{3.12}$$

To ensure the condition of $\boldsymbol{\nabla}\cdot\mathbf{B} = 0$, these averages must be carried out under the nontrivial constraint that defect lines do not start nor stop inside the sample, given in Eq.3.8.

Utilizing this constraint to explicitly eliminate t_d^L in favor of δn_d and re-expressing the strain tensor w_{ij} in terms of the longitudinal and transverse single-valued lattice displacements

$$u_L(\mathbf{q}) = \hat{\mathbf{q}}_\perp \cdot \mathbf{u}(\mathbf{q}) \ , \tag{3.13}$$

$$u_T(\mathbf{q}) = (\hat{\mathbf{z}}\times\hat{\mathbf{q}}_\perp)\cdot\mathbf{u}(\mathbf{q}) \ , \tag{3.14}$$

which are the independent finite wavevector elastic degrees of freedom in the bulk, we obtain the total free energy characterizing the supersolid

$$\begin{aligned} F_{ss} = \int \frac{d^3\mathbf{q}}{(2\pi)^3}\Bigg\{ & \frac{1}{2}\Gamma_T(\mathbf{q})|u_T(\mathbf{q})|^2 + \frac{1}{2}\Gamma_L(\mathbf{q})|u_L(\mathbf{q})|^2 \\ & + \frac{1}{2n_0^2}\Big[\left(\chi^{-1} + K\frac{q_z^2}{q_\perp^2}\right)|\delta n_d(\mathbf{q})|^2 + K|t_d^T(\mathbf{q})|^2\Big] \\ & + \frac{i}{n_0}\Big[\left(\gamma q_\perp - \gamma'\frac{q_z^2}{q_\perp}\right)\delta n_d(\mathbf{q}) u_L(-\mathbf{q}) \\ & + \gamma' q_z t_d^T(\mathbf{q}) u_T(-\mathbf{q})\Big]\Bigg\} \ . \end{aligned} \tag{3.15}$$

In the above we have defined the transverse and longitudinal wavevector-dependent stiffnesses

$$\Gamma_T(\mathbf{q}) = c_{66}q_\perp^2 + c_{44}q_z^2 \ , \tag{3.16}$$

$$\Gamma_L(\mathbf{q}) = c_{11}q_\perp^2 + c_{44}q_z^2 \ . \tag{3.17}$$

and not surprisingly found that the transverse and the longitudinal degrees of freedom decouple. After re-expressing the $S(\mathbf{q})$ and $T_T(\mathbf{q})$ in Eqs.3.10 and 3.11 in terms of these same independent degrees of freedom, these correlation can be easily computed by inverting the corresponding 2×2 matrices that can be read off from the expression for F_{ss}, Eq.3.15. For the structure function of the supersolid we thereby obtain

$$\begin{aligned} S^{ss}(q_\perp, q_z) &= \frac{1}{V}\langle | - in_0 q_\perp u_L(\mathbf{q}) + \delta n_d(\mathbf{q})|^2\rangle \ , \\ &= n_0^2 k_B T q_\perp^2 \frac{(c_{11}q_\perp^2 + c_{44}q_z^2) + (\chi^{-1}q_\perp^2 + Kq_z^2) + 2(\gamma q_\perp^2 - \gamma' q_z^2)}{(c_{11}q_\perp^2 + c_{44}q_z^2)(\chi^{-1}q_\perp^2 + Kq_z^2) - (\gamma q_\perp^2 - \gamma' q_z^2)^2} \ . \end{aligned} \tag{3.18}$$

Similarly, the transverse part of the tilt correlation function is given by

$$T_T^{ss}(q_\perp, q_z) = \frac{1}{V}\langle |in_0 q_z u_T(\mathbf{q}) + t_d^T(\mathbf{q})|^2\rangle \ ,$$
$$= \frac{k_B T n_0^2}{K} + k_B T n_0^2 \frac{q_z^2(1-\gamma'/K)^2}{q_\perp^2 c_{66} + q_z^2(c_{44} - \gamma'^2/K)}. \tag{3.19}$$

It is convenient to define defect-renormalized elastic constants that characterize the effective elastic properties of supersolids. One choice of such a definition, that naturally arises in experiments which measure fluctuations in the *total* magnetic induction $\mathbf{B}$ (e.g., neutron scattering experiments), is in terms of the static correlation functions given in Eqs.3.18 and 3.19, identified with their defect-free lattice counterparts, Eqs.2.14 and 2.15

$$\frac{n_0^2 k_B T}{c_{11}^R(q_\perp)} \equiv S^{ss}(q_\perp, q_z = 0) \ , \tag{3.20}$$

and

$$\frac{n_0^2 k_B T}{c_{44}^R(q_z)} \equiv T_T^{ss}(q_\perp = 0, q_z) \ . \tag{3.21}$$

Similarly, the effective shear modulus c_{66}^R of the supersolid can be defined in terms of another equilibrium equal-time correlation function

$$\frac{k_B T}{c_{66}^R(q_\perp)} \equiv V^{-1}\left[\langle w_{ij}(\mathbf{q}) w_{ij}(-\mathbf{q})\rangle - \langle w_{ii}(\mathbf{q}) w_{jj}(-\mathbf{q})\rangle\right]\Big|_{q_z=0} \ ,$$
$$= V^{-1} q_\perp^2 P_{ij}^T(\hat{\mathbf{q}}_\perp)\langle u_i(\mathbf{q}) u_j(-\mathbf{q})\rangle|_{q_z=0} \ ,$$
$$= V^{-1} q_\perp^2 \langle |u_T(\mathbf{q})|^2\rangle\Big|_{q_z=0} \ . \tag{3.22}$$

which can be easily evaluated by performing a Gaussian thermal average with the free energy functional, Eq.3.15 in the Boltzmann weight. Using Eqs.3.18 and 3.19 together with the definitions, Eqs.3.20 and 3.21, we find

$$c_{11}^R(q_\perp) = \frac{c_{11}\chi^{-1} - \gamma^2}{c_{11} + \chi^{-1} + 2\gamma} \ , \tag{3.23}$$

and

$$c_{44}^R(q_z) = \frac{c_{44} K - \gamma'^2}{c_{44} + K - 2\gamma'} \ . \tag{3.24}$$

From these expressions we observe that for vanishing couplings $\gamma = \gamma' = 0$, the effective elastic moduli of the supersolid are the corresponding moduli of the lattice and the liquid of defects, added in "parallel" — a physically appealing result. For weak coupling this implies that the effective bulk and tilt moduli of the supersolid are always *smaller* than or equal to the minimum of the corresponding moduli of the two subsystems, the lattice and the defects. Hence we find that for γ, γ' small compared to the elastic moduli of the lattice and the defects, fluctuations of vacancy and interstitial densities always *reduces* the effective longitudinal and tilt moduli of the supersolid, relative to that of the defect-free crystal.

The typical behavior of the supersolid bulk modulus c_{11}^R for $c_{11} \neq \chi^{-1}$ as a function of γ is displayed in Fig.4 (c_{44}^R behaves similarly as function of γ'). The figure shows that the supersolid modulus grows (decreases) linearly with positive (negative) coupling, at weak coupling. At an intermediate *positive* value of γ, it reaches a maximum at the value of the smallest of the moduli for the two subsystems. In the strong coupling regime (both positive and negative) the effective modulus decreases, vanishes and even changes sign, indicating an instability in the quadratic model of the supersolid. In our model, this instability is a signal of a (spurious) phase transition *within* the supersolid phase, which in the case of the bulk modulus c_{11}^R, corresponds to additional proliferation of defects and change in the *lattice* density. However, as we show in Appendix A, for a physical vortex supersolid, the elastic moduli $(c_{66}, c_{11}, c_{44}, \chi, K, \gamma, \gamma')$ that appear in our model are constrained to lie outside of this unstable range. In the special degenerate case of $c_{11} = \chi^{-1}$, the effective bulk modulus of the supersolid behaves as $c_{11}^R = (c_{11} + \gamma)/2$, with an analogous result for the tilt modulus c_{44}^R.

The calculation of c_{66}^R, as defined in Eq.3.22, shows that, not surprisingly, vacancy and interstitial density *fluctuations* do *not* renormalize the shear modulus, and

$$c_{66}^R(q_\perp) = c_{66} \ . \tag{3.25}$$

In contrast to dislocations (to be considered in the next section), vacancies and interstitials are unable to relieve a shear stress.

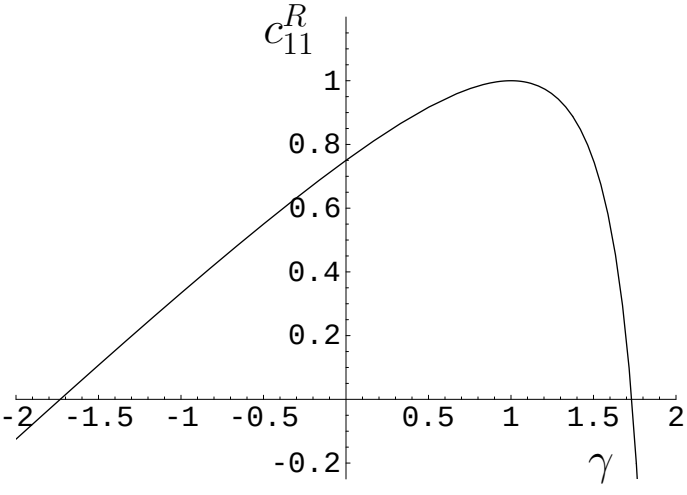

Fig.4.The behavior of the supersolid bulk modulus as function of the coupling γ between the elastic and the defect degrees of freedom, for $c_{11} = 1 < \chi^{-1}$.

The presence of vacancy and interstitial defects also alters the response to a transverse magnetic field. The long wavelength limit of the transverse part of the tilt correlation function, $T_T^{ss}(q_\perp, q_z)$, remains nonanalytic, as in a defect-free crystal, and yields

$$\lim_{q_z \to 0} \chi_T^{ss}(q_\perp = 0, q_z) = -\frac{1}{4\pi}\Big[1 - \frac{B^2}{4\pi c_{44}^R}\Big] , \tag{3.26}$$

$$\lim_{q_\perp \to 0} \chi_T^{ss}(q_\perp, q_z = 0) = -\frac{1}{4\pi}\Big[1 - \frac{B^2}{4\pi K}\Big] . \tag{3.27}$$

Since, as discussed above, these defects soften the lattice by *decreasing* both the longitudinal and tilt moduli the penetration of a transverse field is *enhanced*, as seen from Eq.3.26. A more dramatic effect of the defects is the presence of the second term on the right hand side of Eq.3.27. In the vortex supersolid vacancy and interstitial defects allow flux-line wandering and entanglement, and as a result there is no perfect screening of weak transverse fields uniform along the z axis, and consequently the phase does not exhibit longitudinal superconductivity. The supersolid is both crystalline ($c_{66} \neq 0$) and entangled ($T_T^{ss}(q_\perp, q_z = 0) \neq 0$), as argued by Frey, et al.[20] and consistent with nonvanishing winding correlation function

$$\langle W^2 \rangle = \lim_{q_\perp \to 0} T_T(q_\perp, q_z = 0) , \tag{3.28}$$

$$= \frac{k_B T n_0^2}{K} , \tag{3.29}$$

We stress that the definitions of the effective elastic moduli characterizing a vortex supersolid is far from unique. This is related to the variety of experiments that probe *different* physical properties of the vortex supersolid. Instead of the correlation functions $S^{ss}(\mathbf{q})$ and $T_{ij}^{ss}(\mathbf{q})$ defined in Eqs.3.10 and 3.11, we could have instead focused on

$$\tilde{S}^{ss}(\mathbf{q}) = \frac{n_0^2}{V}\langle |w_{ii}(\mathbf{q})|^2 \rangle , \tag{3.30}$$

$$\tilde{T}_{ij}^{ss}(\mathbf{q}) = \frac{n_0^2}{V}\langle w_{zi}(\mathbf{q}) w_{zj}(-\mathbf{q}) \rangle , \tag{3.31}$$

which probe only fluctuations in the *lattice* positions and *not* the *total vortex* density (related to magnetic induction $\mathbf{B}$). These latter correlation functions are more difficult to probe in a physical experiment, but can be straightforwardly measured in a numerical simulation. Making the identification between the effective elastic moduli of the supersolid and the corresponding correlation functions, in analogy with Eqs.3.20 and 3.21, we define

$$\frac{n_0^2 k_B T}{\tilde{c}_{11}^R(q_\perp)} \equiv \tilde{S}^{ss}(q_\perp, q_z = 0) , \tag{3.32}$$

and

$$\frac{n_0^2 k_B T}{\tilde{c}_{44}^R(q_z)} \equiv \tilde{T}_T^{ss}(q_\perp = 0, q_z) . \tag{3.33}$$

Simple computation of $\tilde{S}^{ss}(\mathbf{q})$ and $\tilde{T}_T^{ss}(\mathbf{q})$, together with these definitions leads to[43]

$$\tilde{c}_{11}^R = c_{11} - \gamma^2 \chi , \tag{3.34}$$

$$\tilde{c}_{44}^R = c_{44} - \frac{\gamma'^2}{K} , \tag{3.35}$$

$$\tilde{c}_{66}^R = c_{66} . \tag{3.36}$$

Another experimentally relevant way to probe elastic properties of vortex supersolids is through the linear response to a constant stress $\sigma_{\alpha j}$ applied at the boundaries of the system. For simplicity, we confine our discussion here to a two-dimensional stress σ_{ij} applied to a boundary lying in the xy-plane. To study the response, we first need to decide to which physical quantity does such stress couple. In a defect-free crystal, the answer is simple: the stress σ_{ij} couples to the lattice strain u_{ij}. In a supersolid, there is, however, a number of possibilities, depending on the nature of the experiment one seeks to describe (as was the case with the correlation functions discussed above). In a real (as opposed to a numerical) experiment the stress on the vortex lattice is produced through an electromagnetic interaction and therefore couples to the magnetic induction, which involves *both* the elastic lattice strain tensor and the defect contribution. Arguments similar to those found in Ref. 39 indicate that the linear response of the supersolid can be studied by adding to the free energy F_{ss} in Eq.3.15 a part due to the external stress,

$$F_\sigma = -\int d\mathbf{r}\, \sigma_{ij}(u_{ij} - \frac{1}{2n_0}\delta_{ij}\delta n_d) , \tag{3.37}$$

and then by minimizing it with respect to the independent elastic strain and defect degrees of freedom.

Before proceeding with the calculation, some remarks are in order. Invoking the fluctuation-dissipation theorem, one might naively conclude that such a static response function is identical to the corresponding equal-time correlation function $S^{ss}(\mathbf{q})$, Eq.3.10 that we studied above. However, this is in fact not the case, in general, even for a defect-free crystal. To understand this difference, we consider for simplicity the case of a two-dimensional crystal. Bulk correlation functions probe the fluctuations of the bulk degrees of freedom at finite (albeit small) wavevector. The *elastic* degrees of freedom of the lattice or supersolid are the *two* components of the lattice displacement (phonons), $u_x(\mathbf{q})$ and $u_y(\mathbf{q})$ (or equivalently $u_L(\mathbf{q})$ and $u_T(\mathbf{q})$). Hence in the definition of $S^{ss}(\mathbf{q})$, Eqs.3.10 and 3.30, the average is over the *two* lattice displacements (as well as over the defects), *not* the components of the strain tensor, $w_{\alpha i}$, which can be written as derivatives of the displacements and therefore are not independent degrees of freedom. In contrast, the response functions, that most directly relate to experimental probes of elasticity, measure the response to

a (often *uniform*) stress applied at the *boundary* of the solid. The corresponding $q = 0$, uniform deformations are described by *three* zero-mode independent degrees of freedom, corresponding to three macroscopic strains u_{xx}, u_{yy} and u_{xy} that can be independently induced in a solid. As a consequence, for a supersolid (or a crystal in general) the equal-time correlation functions differ from the corresponding static response functions, as we now explicitly demonstrate.

Finally, we note that the situation is different in a liquid, where dislocations have proliferated and act as additional degrees of freedom. The proliferated dislocations lead to multi-valued lattice displacements and thereby allow for a *transverse* part of the strain w_{ij}, which (for the first index i), is forbidden in the supersolid. As a result, in a two-dimensional liquid, all *three* components of the symmetric strain (u_{xx}, u_{yy} and u_{xy}) are independent degrees of freedom.

Returning to the derivation of the linear response to a perturbation described by Eq. 3.37, we treat u_{ij}, w_{zj} and the defect densities as independent degrees of freedom and minimize the total free energy, $F_{tot} = F_{ss} + F_\sigma$, with respect to them, to obtain

$$\begin{aligned}
\frac{\delta F_{tot}}{\delta u_{ij}} &= 2c_{66}u_{ij} + \delta_{ij}(c_{11} - 2c_{66})u_{kk} + \delta_{ij}\frac{\gamma}{n_0}\delta n_d - \sigma_{ij} \ , \\
&= 0 \ , \qquad (3.38) \\
\frac{\delta F_{tot}}{\delta w_{zj}} &= c_{44}w_{zj} + \frac{\gamma'}{n_0}t_{dj} \ , \\
&= 0 \ , \qquad (3.39) \\
\frac{\delta F_{tot}}{\delta n_d} &= \frac{\chi^{-1}}{n_0^2}\delta n_d + \frac{\gamma}{n_0}u_{kk} + \frac{1}{2n_0}\delta_{ij}\sigma_{ij} \ , \\
&= 0 \ , \qquad (3.40) \\
\frac{\delta F_{tot}}{\delta t_{di}} &= Kt_{di} + \frac{\gamma'}{n_0}w_{zi} \ , \\
&= 0 \ . \qquad (3.41)
\end{aligned}$$

Given that the applied stress σ_{ij} is purely within the xy-plane equations (3.39) and (3.41) give

$$t_{di} = 0 \ , \qquad (3.42)$$

$$w_{zi} = 0 \ , \qquad (3.43)$$

and the response is z independent. Solving the remaining equations for the strain and the defect density, we find

$$u_{kk} = \frac{1 + \gamma\chi}{2(c_{11} - c_{66} - \gamma^2\chi)}\,\sigma_{kk} \ , \qquad (3.44)$$

$$\frac{\delta n_d}{n_0} = -\frac{\chi(c_{11} - c_{66} + \gamma)}{2(c_{11} - c_{66} - \gamma^2\chi)}\,\sigma_{kk} \ , \qquad (3.45)$$

which, when used inside Eq.3.38 give

$$u_{ij} = R^{ss}_{ij,kl}\sigma_{kl} \ , \qquad (3.46)$$

where $R^{ss}_{ij,kl}$ is the *uniform* static response function given by

$$\begin{aligned}
R^{ss}_{ij,kl} &= \frac{(2c_{66} - c_{11})(1 + \gamma\chi) + 2\gamma\chi(c_{11} - c_{66} + \gamma)}{4c_{66}(c_{11} - c_{66} - \gamma^2\chi)}\,\delta_{ij}\delta_{kl} \\
&\quad + \frac{1}{2c_{66}}\delta_{ik}\delta_{jl} \ . \qquad (3.47)
\end{aligned}$$

As a check we observe that for $\chi \to 0$, which freezes out the defects, $R^{ss}_{ij,kl}$ reduces to the well-known response function for a defect-free crystal[40]

$$\begin{aligned}
R^{crystal}_{ij,kl} &= \frac{(2c_{66} - c_{11})}{4c_{66}(c_{11} - c_{66})}\,\delta_{ij}\delta_{kl} \\
&\quad + \frac{1}{2c_{66}}\delta_{ik}\delta_{jl} \ . \qquad (3.48)
\end{aligned}$$

Consistent with our discussion above, $R^{ss}_{ij,kl}$ differs from the corresponding $q_z = 0$ equal-time correlation function, computed with the lattice displacements as the independent degrees of freedom.

Using Eqs.3.46 and 3.47 we can now compute the response to any uniform stress, σ_{ij}. For example, a uniform hydrostatic pressure δp corresponds to

$$\sigma_{ij} = -\delta p\delta_{ij} \ , \qquad (3.49)$$

and we obtain the bulk modulus for the vortex supersolid as

$$\begin{aligned}
\frac{1}{B_{ss}} &\equiv -\frac{1}{A}\frac{\delta A}{\delta p} \ , \\
&= \frac{1}{n_0}\frac{\delta n}{\delta p} \ , \\
&= -\frac{u_{kk}}{\delta p} + \frac{1}{n_0}\frac{\delta n_d}{\delta p} \ , \\
&= \frac{B + \chi^{-1} + 2\gamma}{B\chi^{-1} - \gamma^2} \ , \qquad (3.50)
\end{aligned}$$

where $B = c_{11} - c_{66}$ is the standard definition for a defect-free crystal bulk modulus. We note the similarity in form with the correlation function $S^{ss}(\mathbf{q}_\perp, q_z = 0)$, that we used to define c_{11}^R, Eq.3.20. As discussed above, the computation of the uniform static *response function* gives the *bulk modulus*, $c_{11} - c_{66}$, while the equal-time correlation function (at $q_z = 0$) defines the longitudinal phonon modulus, c_{11}.

As we observed above for the effective c_{11}^R in Eq.3.24, here too in the absence of interaction between the defects and the lattice ($\gamma = 0$), the supersolid bulk modulus is simply determined by the bulk moduli of the two systems, added in parallel, $B_{ss}^{-1} = B^{-1} + \chi$.

Significant caution must be applied in comparing expression (3.50) with experiments. If, for example, the compression is performed on a time scale that is slow compared to the relaxation time of the elastic degrees of freedom, but fast compared to that of the defects (which, being a conserved "charge" density, relaxes only diffusively), then the defects are effectively frozen on the time scale of the experiment. In this case, corresponding to

$\chi = 0$, only elastic degrees of freedom can respond and the result for B_{ss} is simply B of the defect-free crystal.

The vortex supersolid shear modulus c_{66}^{ss} can be probed by applying a constant force normal to two opposite lateral boundaries of a rectangular xy-crossection sample. The corresponding stress is given by

$$\sigma_{ij} = \sigma \delta_{ix} \delta_{jx} \ . \tag{3.51}$$

Such stress induces both the longitudinal (u_L) and the transverse (u_T) deformations of the lattice. The shear modulus is defined in terms of the normal strain, $u_{xx} - u_{yy}$, as

$$\frac{1}{c_{66}^{ss}} = 2\frac{u_{yy} - u_{xx}}{\sigma} \ . \tag{3.52}$$

Consistent with our earlier calculation that used equal-time correlation function, we find here that

$$c_{66}^{ss} = c_{66} \tag{3.53}$$

i.e., the shear modulus remains unrenormalized by fluctuations in density of vacancies and interstitials.

IV. DISLOCATION LOOPS IN A VORTEX SUPERSOLID: A MODEL OF VORTEX LIQUID

We now turn to the description of a vortex liquid. This is a disordered, dissipative state of the flux-line array, that results from either a direct melting of a defect-free vortex crystal or (possibly) a continuous melting[13] of a vortex supersolid, discussed in previous sections.

Following ideas of Kosterlitz and Thouless,[14] extended in Ref. 16 to three-dimensional vortex systems, we describe a flux-line liquid as a supersolid with a finite equilibrium concentration of unbound dislocation loops and vacancy/interstitial defect lines. Such an approach nicely complements the more conventional hydrodynamic description of the vortex liquid studied in Refs. 37,36. While somewhat more involved, the advantage of the approach taken here is that it provides a more direct connection between the vortex liquid and vortex *ordered* phases (crystals), in which the defects are bound, thereby presenting a unified description. It also provides a valuable detailed *"microscopic"* characterization of the distinction between vortex liquids and solids.

The properties of a flux-line lattice in the presence of an unbound gas of dislocation loops, but no vacancies nor interstitials, were studied in Ref. 16. In the absence of vacancy and interstitial defects, dislocation loops are constrained to lie in a plane spanned by their Burger's vector and the z axis. These planar dislocation loops can only relax applied stresses by "gliding" along the z axis. Clearly, once dislocation loops proliferate on all scales, vacancies and interstitials will also unbind and *both* of these defects will exist in the resulting bond-orientationally ordered liquid. The goal of this section is to incorporate vacancies and interstitials into a complete description of a vortex liquid. We will explicitly demonstrate that a finite concentration of vacancy and interstitial defects allows for "climb-like" distortions of dislocation loops, which can move out of the $\hat{\mathbf{z}}$-$\mathbf{b}$ plane by absorbing and emitting vacancies and interstitials.

A. Model

To construct a complete model of a vortex liquid we now proceed to incorporate dislocation loops into the model of a supersolid, presented in Sec.III. We do this by allowing multi-valued lattice displacement fields, $\mathbf{u}$. The loop integral of $\mathbf{u}$,

$$\oint du_i(\mathbf{r}) = -b_i(\mathbf{r}) \ , \tag{4.1}$$

enclosing a dislocation line, fails to close by a Burger's lattice vector, $\mathbf{b}$. The direction of integration around the contour is that of a right-handed screw advancing parallel to a unit tangent vector $\boldsymbol{\tau}$ to the dislocation line. The peculiarity of dislocation in a lattice of z-directed lines is that while the Burger's vector is two-dimensional and by definition lies in the xy plane, the tangent $\boldsymbol{\tau}$ to the defect line is a three-dimensional vector.[16,41]

To study properties of the system on scales that are long compared to the spacing between dislocation lines, we use a continuum description. We consider a small hydrodynamic volume and introduce the Burger's "charge" density *tensor* $\alpha_{\beta j}(\mathbf{r})$, whose integral over an open surface S, gives the total Burger's vector of dislocation lines directed along the surface normal n_β and enclosed by a contour C bounding the surface,

$$\int_S \alpha_{\beta j} n_\beta dA = \sum_n b_j^{(n)} \ . \tag{4.2}$$

For a single dislocation line, directed along the tangent τ_β, with Burger's vector b_i, the defect density tensor is given by $\alpha_{\beta i} = \tau_\beta b_i \delta^{(2)}(r_\perp)$. The rectangular (3×2) density tensor $\alpha_{\beta j}(\mathbf{r})$ is therefore a measure of the number of dislocation lines with Burger's vector b_j crossing a unit area normal to the dislocation tangent τ_β. We remind the reader that Roman letters $i, j, k, ...$ are used to denote indices that run only over the values x and y, and Greek letters $\alpha, \beta, \gamma, ...$ are reserved for indices that run over the three-dimensional set x, y, z.

By definition, dislocations in the z-directed line crystal must have their Burger's vectors lie in the xy plane. Consequently the three-dimensional vector $\alpha_{zj}(\mathbf{r})$, $(j = x, y)$ describes z-directed edge dislocations. Edge dislocations lying in the xy plane are described by the antisymmetric part of the two-dimensional tensor $\alpha_{ij}^{\perp}(\mathbf{r})$, $(i = x, y$ and $j = x, y$, with $\alpha_{\beta j} = (\alpha_{ij}^{\perp}, \alpha_{zj}))$. In the *absence* of vacancies and interstitials, however, these type of xy-plane-directed edge dislocations correspond to a branching or

merging of flux lines, which necessarily involve fractional or double flux-"charged" vortex lines, both energetically forbidden. In contrast, vacancies and interstitials allow for this type of edge dislocations, as we will demonstrate below. Screw dislocations, on the other hand always run normal to flux lines, i.e., they lie in the xy plane, and lead to entanglement of the vortex lines.[42] They are described by the *symmetric* part of $\alpha^{\perp}_{ij}(\mathbf{r})$.

By rewriting Eq.4.1 in differential form and then averaging the resulting equation over a hydrodynamic volume, containing many dislocation lines, we relate the dislocation density tensor $\alpha_{\beta j}(\mathbf{r})$ to the local lattice strain $w_{\beta j}(\mathbf{r})$,

$$\epsilon_{\alpha\beta\gamma}\partial_\beta w_{\gamma k}(\mathbf{r}) = -\alpha_{\alpha k}(\mathbf{r}) \ . \tag{4.3}$$

Hence in the presence of dislocations ($\alpha_{\beta j} \neq 0$), the strain tensor $w_{\beta j}$ contains a singular part that cannot be written as a gradient (∂_β) of a single-valued displacement field u_j. Finally, dislocation loops must either close or terminate at sample boundaries. This amounts to the condition

$$\partial_\beta \alpha_{\beta j}(\mathbf{r}) = 0 \ . \tag{4.4}$$

We now proceed to incorporate the dislocation degrees of freedom into the model of the supersolid studied in Sec.III. We first recall that the fluctuations of the local magnetic induction $\delta\mathbf{B} = (\mathbf{B}_\perp, \delta B_z)$ are related to the changes in density and orientation of flux lines, with contributions from both local strains and vacancy and interstitial defects. In the long wavelength limit these relations are obtained by inserting δn and $\mathbf{t}$ given by Eqs.3.6 and 3.7 in Eqs.2.4 and 2.5,

$$\delta B_z = \phi_0[-n_0 w_{ii}(\mathbf{r}) + \delta n_d(\mathbf{r})] \ , \tag{4.5}$$

$$\delta B_{\perp i} = \phi_0[n_0 w_{zi}(\mathbf{r}) + t_{di}(\mathbf{r})] \ . \tag{4.6}$$

In the presence of dislocations, the strain tensor $w_{\alpha j}$ is given by the sum of a regular, longitudinal (on first, Greek index) part, defined in Eq.2.3 in terms of the derivatives of a single-valued displacement field u_j, and a singular, transverse (on the first, Greek index) part, $w^{\rm s}_{\alpha i}$, due to dislocations

$$w_{\alpha j} = \partial_\alpha u_j + w^{\rm s}_{\alpha j} \ . \tag{4.7}$$

By imposing the $\boldsymbol{\nabla}\cdot\mathbf{B} = 0$ condition and using Eqs.4.5 and 4.6, we obtain

$$\partial_z \delta n_d + \boldsymbol{\nabla}_\perp \cdot \mathbf{t}_d = -n_0(-\partial_z w^{\rm sing}_{ii} + \partial_i w^{\rm sing}_{zi}) \ . \tag{4.8}$$

It is important to note that, in contrast to the defect-free crystal and the supersolid, where the *elastic* part $w_{\beta j}$ ($\partial_\beta u_j$) identically satisfies $\boldsymbol{\nabla}\cdot\mathbf{B} = 0$, here this condition imposes a nontrivial constraint that couples dislocations and vacancy-interstitial defects. This becomes apparent by using Eq.4.3 to eliminate $w_{\beta j}$ from the constraint in favor of the dislocation density tensor, with the result

$$\partial_z \delta n_d + \boldsymbol{\nabla}_\perp \cdot \mathbf{t}_d = n_0 \epsilon_{ij}\alpha^{\perp}_{ij}(\mathbf{r}) \ . \tag{4.9}$$

This important condition is one of the main results of our work and is an essential ingredient in the complete "elastic" description of the vortex liquid state. We first note that in the supersolid phase, where dislocation loops are bound and lattice displacements are singe-valued, $\alpha_{\beta j} = 0$, and the constraint reduces to the vacancy-interstitial line continuity condition, Eq.3.8. On the other hand, in a description of a vortex liquid which ignores vacancies and interstitials it reduces to the $\epsilon_{ij}\alpha^{\perp}_{ij} = 0$ condition of Ref. 16, enforcing the constraint, discussed above, that in the absence of vacancies and interstitials, dislocation loops are confined to lie in the plane defined by their Burger's vector and the average external magnetic field. In the presence of vacancies and interstitials Eq.4.9 explicitly demonstrates that these defects provide a mechanism by which the dislocation loop can effectively climb out of this plane. They do this by emitting or absorbing vacancy and interstitial line defects. The allowance of *nonplanar* dislocation loops in vortex supersolids and liquids then removes the artificial condition of a vanishing antisymmetric part of the dislocation density tensor and in general $\epsilon_{ij}\alpha^{\perp}_{ij} \neq 0$ in these phases. As anticipated above, this allows xy-plane-directed *edge* dislocations to proliferate upon melting.

The above constraint, Eq.4.9, is one way that the additional degrees of freedom associated with proliferated dislocations enter the description of the vortex liquid. Dislocations of course also contribute directly through the "elastic" free energy in a way that we now derive.

The free energy F of a lattice with dislocations and vacancy/interstitial defects is given by $F_{ss} = F_{\rm latt} + F_d + F_{int}$, but with derivatives of the phonon field replaced by the total strain tensor given in Eq. 4.7, i.e.,

$$\begin{aligned} F = \frac{1}{2}\int d\mathbf{r} w_{\alpha i} C_{\alpha i\beta j} w_{\beta j} \\ + \frac{1}{2n_0^2}\int d\mathbf{r}\big[\chi^{-1}(\delta n_d)^2 + K(\mathbf{t}_d)^2\big] \\ + \frac{1}{n_0}\int d\mathbf{r}\big[\gamma w_{ii}\delta n_d + \gamma' w_{zi} t_{di}\big] \\ + F_{\rm core}, \end{aligned} \tag{4.10}$$

To make the notation more compact, the purely elastic part of the free energy, given by the first term on the right hand side of Eq. 4.10, has been written in terms of the elastic tensor,

$$\begin{aligned} C_{\alpha i\beta j} = c_{66}(\delta_{\alpha\beta} - \delta_{\alpha z}\delta_{\beta z})\delta_{ij} + c_{66}\delta_{\alpha j}\delta_{\beta i} \\ + (c_{11} - 2c_{66})\delta_{\alpha i}\delta_{\beta j} + c_{44}\delta_{\alpha z}\delta_{\beta z}\delta_{ij} \ . \end{aligned} \tag{4.11}$$

We have also added to the free energy of the defective lattice a term $F_{\rm core}$ representing the core energy of the dislocations, given by

$$F_{\rm core} = \int d\mathbf{r}[E_e\alpha^2_{zi} + E_s\alpha^2_{ii} + E'_s\alpha_{ij}\alpha_{ij} + E'_e(\epsilon_{ij}\alpha_{ij})^2]. \tag{4.12}$$

The core energy $F_{\rm core}$ has been written on the basis of symmetry considerations. It incorporates terms accounting for the edge and screw dislocation core energies per unit length, E_e, E'_e, E_s and E'_s. As discussed in Ref. 16, although $E'_e = E'_s = 0$ for a single dislocation line, nonzero values of E'_e and E'_s are required to describe short range interactions in the hydrodynamic limit. The values for the core energies are estimated to be $E_e \simeq c_{66}b^2$, $E_s \simeq E'_s \simeq \sqrt{c_{66}c_{44}}\,b^2$ and $E'_e \simeq \sqrt{c_{11}c_{44}}\,b^2$.[16]

While the elastic part ($\partial_\alpha u_i$) of the strain tensor identically satisfies Eq.4.3, the singular part is found by "inverting" this equation in Fourier space. This gives

$$w^{\rm s}_{\alpha j}(\mathbf{q}) = -\frac{i}{q^2}\epsilon_{\alpha\beta\gamma}q_\beta\alpha_{\gamma j}(\mathbf{q}) + iq_\alpha\psi_j(\mathbf{q})\ , \tag{4.13}$$

where ψ_j is an arbitrary function, reflecting the fact that the solution to Eq.4.3 is only determined up to an arbitrary longitudinal part. This is analogous to the gauge freedom that appears in electromagnetism (or other gauge theories) when, for example, Maxwell equation $\boldsymbol{\nabla}\cdot\mathbf{E} = \rho$ is solved for the electric field $\mathbf{E}$ in terms of the charge density ρ.

One convenient and natural choice of ψ_j is obtained by requiring that the corresponding $w^{\rm s}_{\alpha j}$ minimizes the total free energy F, Eq.4.10, with respect to lattice displacements. Such a choice is mathematically convenient for computing thermodynamic averages, because it removes all couplings between the phonons u_j and the defect degrees of freedom. Physically, this choice of $w^{\rm s}_{\alpha j}$ corresponds to elastically equilibrated defects.

To compute ψ_i corresponding to this convenient gauge choice, we insert $w_{\alpha i}$, Eq.4.7 into F, Eq.4.10, and require that the *linear* terms in $\mathbf{u}$ vanish, which of course is equivalent to the requirement that $w^{\rm s}_{\alpha i}$ minimizes F. The resulting Euler-Lagrange equation is given by

$$\frac{\delta F}{\delta u_i} = -\partial_\alpha\sigma_{\alpha i} - \frac{\gamma}{n_0}\partial_i\delta n_d - \frac{\gamma'}{n_0}\partial_z t_{di} = 0, \tag{4.14}$$

where

$$\sigma_{\alpha i} = C_{\alpha i\beta j}w_{\beta j} \tag{4.15}$$

is the corresponding stress tensor. The solution is more conveniently written in Fourier space, where it is given by

$$\begin{aligned}\psi_i(\mathbf{q}) = \frac{1}{q^2}\big(A^{-1}\big)_{ij}q_\alpha C_{\alpha j\beta k}\epsilon_{\beta\gamma\eta}q_\gamma\alpha_{\eta k}(\mathbf{q}) \\ + \frac{i}{n_0}\big(A^{-1}\big)_{ij}\big[\gamma q_j\delta n_d(\mathbf{q}) + \gamma' q_z t_{dj}(\mathbf{q})\big].\end{aligned} \tag{4.16}$$

Here A^{-1} is the inverse of a 2×2 matrix A, with $A_{ij} = q_\alpha C_{\alpha i\beta j}q_\beta$. Its elements are given by,

$$\big(A^{-1}\big)_{ij} = \frac{1}{\Gamma_T(\mathbf{q})}\left[\delta_{ij} - \frac{(c_{11}-c_{66})}{\Gamma_L(\mathbf{q})}q_{\perp i}q_{\perp j}\right], \tag{4.17}$$

where $\Gamma_T(\mathbf{q})$ and $\Gamma_L(\mathbf{q})$ are the transverse and longitudinal elastic elastic stiffnesses, defined in Eqs. 3.16, 3.17.

With this choice of ψ_i, by construction, the total free energy breaks up into two parts

$$F = F_{\rm latt} + F_{\rm def}, \tag{4.18}$$

where $F_{\rm latt}$ is the defect-free elastic part of the free energy given in Eq. 2.1 and rewritten here for convenience in Fourier space,

$$F_{\rm latt} = \frac{1}{2}\int\frac{d^3\mathbf{q}}{(2\pi)^3}\Big[\Gamma_T(\mathbf{q})|u_T(\mathbf{q})|^2 + \Gamma_L(\mathbf{q})|u_L(\mathbf{q})|^2\Big]\ . \tag{4.19}$$

This involves only phonons degrees of freedom, as for a defect-free crystal. The second, defect part, $F_{\rm def}$, is the free energy of an interacting gas of dislocation loops and vacancy-interstitial line-defects. It is given by

$$\begin{aligned}F_{\rm def} = \frac{1}{2}\int d\mathbf{r}w^s_{\alpha i}C_{\alpha i\beta j}w^s_{\beta j} \\ + \frac{1}{2n_0^2}\int d\mathbf{r}\big[\chi^{-1}(\delta n_d)^2 + K(\mathbf{t}_d)^2\big] \\ + \frac{1}{n_0}\int d\mathbf{r}\big[\gamma w^s_{ii}\delta n_d + \gamma' w^s_{zi}t_{di}\big],\end{aligned} \tag{4.20}$$

where $w^s_{\alpha i}$ is the singular part of the strain tensor, given by Eqs. 4.13 and 4.16. This defect free energy must be supplemented with the continuity conditions Eq.4.9 and Eq.4.4 for the vacancy/interstitial defect lines and the dislocation lines, respectively. The constraint (4.9) can be directly incorporated into the free energy by using it to explicitly eliminate the *longitudinal* part of the vacancy-interstitial defects tangent vector,

$$t^L_d(\mathbf{q}) \equiv \hat{\mathbf{q}}_\perp\cdot\mathbf{t}_d(\mathbf{q})\ , \tag{4.21}$$

$$= -\frac{q_z}{q_\perp}\delta n_d(\mathbf{q}) - \frac{i}{q_\perp}n_0\epsilon_{ij}\alpha^\perp_{ij}(\mathbf{q})\ , \tag{4.22}$$

in favor of the defect density $\delta n_d(\mathbf{q})$ and the antisymmetric part of the dislocation density tensor $\alpha^\perp_{ij}(\mathbf{q})$. Finally, using Eqs. 4.13 and 4.16 to eliminate the singular strain field in terms of the defect degrees of freedom in Eq. 4.20, we obtain

$$\begin{aligned}F_{\rm def} = \frac{1}{2}\int\frac{d\mathbf{q}}{(2\pi)^3}\Big\{\tilde{R}_{\mu i\nu j}(\mathbf{q})\alpha_{\mu i}(\mathbf{q})\alpha_{\nu j}(-\mathbf{q}) + A(\mathbf{q})\delta n_d(\mathbf{q})\delta n_d(-\mathbf{q}) + C(\mathbf{q})t^T_d(\mathbf{q})t^T_d(-\mathbf{q}) \\ + iD_{\mu i}(\mathbf{q})\Big[\alpha_{\mu i}(-\mathbf{q})\delta n_d(\mathbf{q}) - \alpha_{\mu i}(\mathbf{q})\delta n_d(-\mathbf{q})\Big] + iG_{\mu i}(\mathbf{q})\Big[\alpha_{\mu i}(-\mathbf{q})t^T_d(\mathbf{q}) - \alpha_{\mu i}(\mathbf{q})t^T_d(-\mathbf{q})\Big]\Big\}\ ,\end{aligned} \tag{4.23}$$

where $\mathbf{t}^T_d(\mathbf{q}) = \mathbf{t}_d(\mathbf{q}) - \hat{\mathbf{q}}_\perp t^L_d(\mathbf{q})$ is the transverse part of the defect tangent vector.

The kernels $\tilde{R}_{\mu i,\nu j}(\mathbf{q})$, $A(\mathbf{q})$, $C(\mathbf{q})$, $D_{\mu i}(\mathbf{q})$ and $G_{\mu i}(\mathbf{q})$ depend in a complicated way on the elastic moduli (c_{66}, c_{11}, c_{44}) of the lattice, and on wavevectors $q_\perp$ and q_z, and are given explicitly in Appendix B.

B. Correlations and response functions

In this section we evaluate the renormalization of the elastic constants of the flux-line lattice due to dislocations and vacancy/interstitial defects. The renormalized elastic constants are defined by Eqs. (3.20-3.22), but with the understanding that the correlation functions are now those of a lattice with an equilibrated concentration of defects and dislocations. This means that the structure function and the tilt correlation function are formally given in terms of the strain tensor and the defect fields by the same expressions 3.10 and 3.11 used for the supersolid, but the strain tensor $w_{\alpha i}$ is now the total strain given in Eq. 4.7, including the singular part. The same holds for the correlation function that determined the shear modulus defined on the first line of Eq. 3.22. The brackets in these correlation functions now denote a thermal average with the free energy $F_{\rm latt} + F_{\rm def}$, with $F_{\rm def}$ given by Eq. 4.23. The average is carried out by integrating over all configurations of dislocations, described by the components of the dislocation density tensor, $\alpha_{\beta i}$, and vacancy/interstitial lines, described by the defects density, δn_d, and tilt field, t_d^T. The integration must be done subject to the constraint that dislocation lines are closed, given by Eq. 4.4. The "continuity" constraint for defect lines, expressed by Eq. 4.9, has already been incorporated into the free energy $F_{\rm def}$. The computation of correlation functions is conceptually simple but technically quite involved and was carried out using Mathematica symbolic manipulator program. Only the results will be given here.

The full expression for the density, tilt field, and other correlation functions are too "horrifying" to be shown here, and we therefore only display their long wavelength limits, which determine the renormalized elastic constants, according to Eqs. (3.20-3.22).

The structure factor vanishes as $q_\perp \to 0$, as required by the density sum rule. The renormalized longitudinal modulus as defined by Eq. (3.20) is given by,

$$\frac{1}{c_{11}^R(q_\perp)} = \frac{1}{c_{11}}\left\{1 + \frac{c_{11}[2c_{66}(c_{11}-c_{66}) + c_{11}E_e q_\perp^2] + 2c_{66}^2\chi^{-1} + \gamma(\gamma+2c_{11})(2c_{66}+E_e q_\perp^2)}{\chi^{-1}[2c_{66}(c_{11}-c_{66}) + c_{11}E_e q_\perp^2] - \gamma^2(2c_{66}+E_e q_\perp^2)}\right\}. \tag{4.24}$$

The renormalized tilt modulus defined by Eq. (3.21) is

$$\frac{1}{c_{44}^R(q_z)} = \lim_{q_z\to 0} T_T(q_z, q_\perp = 0) = \frac{c_{44}+K-2\gamma'}{c_{44}K-\gamma'^2}\ . \tag{4.25}$$

We find that in the long wavelength limit both c_{11}^R and c_{44}^R are identical to the elastic constants of a lattice with only vacancy and interstitial defects. In other words, somewhat surprisingly, the coupling of dislocations to vacancy/interstitial defect lines does *not* yield any *additional* renormalization of the tilt and compressional moduli, even if it does make it possible for dislocations to relax stresses by climbing out of the $(\mathbf{b}, \hat{\mathbf{z}})$ plane and allows for (otherwise forbiddingly costly) xy directed edge dislocations. Finally, the renormalized shear modulus is

$$\frac{1}{c_{66}^R(q_\perp)} = \frac{1}{c_{66}} + \frac{1}{E_e q_\perp^2} + \frac{\chi^{-1}c_{11}(c_{11}-2c_{66}) - \gamma^2(c_{11}-4c_{66})}{c_{11}\Big[\chi^{-1}\big(2c_{66}(c_{11}-c_{66}) + c_{11}E_e q_\perp^2\big) - \gamma^2(2c_{66}+E_e q_\perp^2)\Big]}. \tag{4.26}$$

Dislocations renormalize the long wavelength ($q \to 0$) shear modulus to zero, yielding liquid-like response to shear stresses.

We now discuss various limiting cases for our results. In the absence of coupling between the gas of vacancy/interstitial defects and the lattice ($\gamma = 0$, $\gamma' = 0$), the various correlation functions are simply given by the sum of the contributions from a lattice with an equilibrium concentration of unbound dislocations (corresponding to the *constrained* hexatic line liquid discussed by Marchetti and Nelson[16]) and from a liquid of defect lines. The corresponding elastic constants add in parallel, with

$$\Big(\frac{1}{c_{11}^R(q_\perp)}\Big)_{\gamma=\gamma'=0} = \chi + \frac{1}{c_{11}^{\rm MN}}, \tag{4.27}$$

$$\Big(\frac{1}{c_{44}^R(q_\perp)}\Big)_{\gamma=\gamma'=0} = \frac{1}{K} + \frac{1}{c_{44}^{\rm MN}}, \tag{4.28}$$

$$\Big(\frac{1}{c_{66}^R(q_\perp)}\Big)_{\gamma=\gamma'=0} = \frac{1}{c_{66}^{\rm MN}}, \tag{4.29}$$

where we have denoted by the superscript "MN" the elastic constants of a lattice with an equilibrium concentration of unbound dislocations, but with a constraint forbidding vacancy and interstitial defects,[16] given by

$$\frac{1}{c_{11}^{\rm MN}} = \frac{1}{c_{11}}\left[1 + \frac{2c_{66}^2}{2c_{66}(c_{11}-c_{66}) + c_{11}E_e q_\perp^2}\right] \tag{4.30}$$

$$\frac{1}{c_{66}^{\rm MN}} = \frac{1}{c_{66}} + \frac{1}{E_e q_\perp^2} + \frac{(c_{11}-2c_{66})}{2c_{66}(c_{11}-c_{66}) + c_{11}E_e q_\perp^2} \tag{4.31}$$

$$\frac{1}{c_{44}^{\rm MN}} = \frac{1}{c_{44}}. \tag{4.32}$$

The elastic constants of a supersolid, i.e., the lattice with only vacancy and interstitial defects, can be obtained by letting all the dislocation core energies go to infinity ($E_e, E'_e, E_s, E'_s \to \infty$). It is easy to see that in this limit we recover the results discussed in Sec. II. Finally, when $\chi^{-1} \to \infty$ and $K \to \infty$ vacancy and interstitial defects are forbidden and the elastic constants reduce again to those given in Eqs. 4.30-4.32.

We recall that the coupling of dislocations to vacancy and interstitial lines allows dislocations to relax stresses by climbing out of the $(\mathbf{b}, \hat{\mathbf{z}})$ plane via the emission or absorption of vacancies and interstitials – a mechanism for relaxing stresses that is forbidden in the hexatic liquid of Marchetti and Nelson[16].

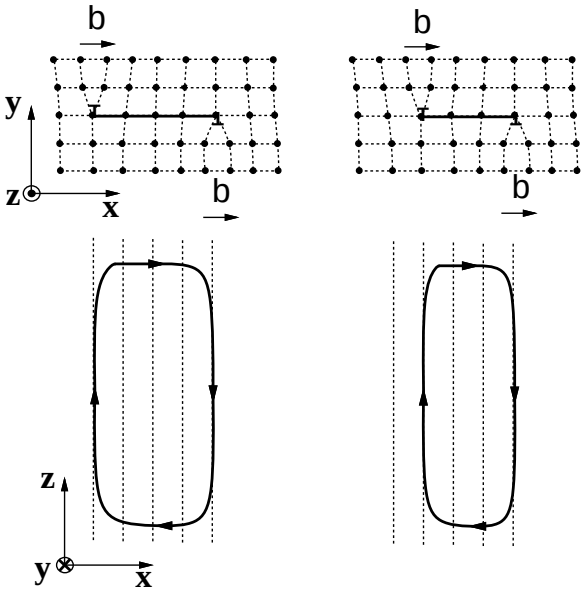

Fig.5. *Gliding* of an edge dislocation loop, allowed even in the absence of vacancies and interstitials. For simplicity we have sketched the dislocation loop for the case of a square lattice. The dotted vertical lines refer to the defect-free square lattice and serve as a guide for the eye.

Figure 5 shows a planar dislocation loop with $\mathbf{b} = b\hat{\mathbf{x}}$ of the type considered by Marchetti and Nelson[16]. This loop lies in its glide plane (the xz plane) and can easily relax a shear by gliding in this plane. The climbing of the same dislocation loop out of its glide plane is described pictorially in Fig.6.

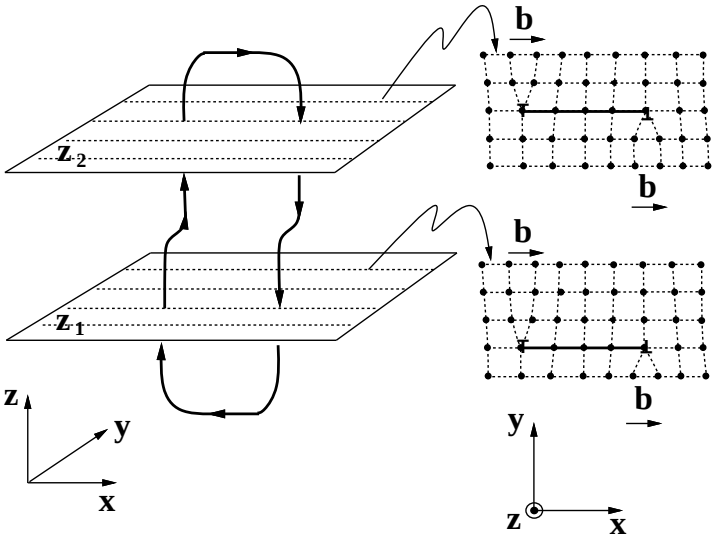

Fig.6. *Climbing* of an edge dislocation loop in a square lattice, only allowed in the presence of vacancies and interstitials. The Burger's vector of the loop is in the $+x$ direction. The lattice configuration at two cross-sections z_1 and z_2 shows the climbing in the y direction, normal to the Burger's vector.

It is clear that climb can only occur via the emission or absorption of vacancy or interstitial defects, as summarized by Eq.4.9. Such climb "motion" can occur in response to the force on the dislocation loop resulting from applying a uniform external tilt to the lattice, corresponding to a constant stress $\sigma^{\rm ext}_{i\alpha} = \delta_{ix}\delta_{\alpha z}\sigma^{\rm ext}_{zx}$. The force on a dislocation line due to a uniform stress $\sigma^{\rm ext}_{i\alpha}$ is the familiar Peach-Köhler force, given by

$$F^{\rm PK}_{\beta} = \epsilon_{\alpha\beta\gamma}\tau_\gamma\sigma^{\rm ext}_{i\alpha}b_i. \tag{4.33}$$

Equation 4.33 differs slightly from the corresponding expression found in textbooks as the stress tensor in a flux-line lattice is not a symmetric (or even a square) matrix. The Peach-Köhler force on the rectangular loop shown in Fig.5 due to a uniform tilt in the xy plane is normal to the plane of the loop (along y) and there is no force on any segment of the loop parallel to z. Specifically, for $\boldsymbol{\tau} = \hat{\mathbf{x}}$, we find $\mathbf{F}^{\rm PK,tilt} = -\sigma^{\rm ext}_{xz}b\hat{\mathbf{y}}$ and for $\boldsymbol{\tau} = -\hat{\mathbf{x}}$, we find $\mathbf{F}^{\rm PK,tilt} = \sigma^{\rm ext}_{xz}b\hat{\mathbf{y}}$. In other words, the Peach-Köhler force acts as a couple and tries to rotate the loop out of its glide plane. The screw components of the loop running along $\pm\hat{\mathbf{x}}$ can glide in any plane that contains them. In particular, they will glide in the $\hat{\mathbf{y}}$ or $-\hat{\mathbf{y}}$ direction under the action of the force. For this to happen the edge sections must climb out of the glide plane by emitting or absorbing vacancies and interstitials, as shown in Fig.6. By gliding out of the sample along the y direction, the screw dislocations can relax a uniform tilt of the lines towards $\pm x$. We note that if one thinks of z as a fictitious time, the constraint 4.9 is formally identical to the temporal continuity equation for the density of point vacancy/interstitial defects, diffusing in the presence of dislocations in a two-dimensional lattice[39]. Dislocations

provide a source of point defects as they climb across the sample. The renormalization of the tilt modulus can therefore occur only when vacancy and interstitial defects are allowed.

It is also instructive to consider the behavior of another typical dislocation loop, shown in Fig.7. This loop has $\mathbf{b} = b\hat{\mathbf{x}}$ and lies in the yz plane. The two edge segments running parallel to z lie in two different and parallel glide planes. The loop is closed by segments running along y which are also edge dislocations in nature, as $\mathbf{b} \perp \boldsymbol{\tau}$.

This is an example of a dislocation loop characterized by $\epsilon_{ij}\alpha_{ij}^{\perp} \neq 0$. Such a loop is not allowed in the absence of vacancy and interstitials, as without such defects the edge segments running along y would require a row of vortex lines to merge or split into single lines carrying twice or half a flux quantum – an energetically forbidding configuration. Denoting by $z_1 < z_2$ the vertical location of the two segments of the loop running along y, we can understand the existence of the loop as arising from a set of interstitial defects that are randomly distributed in the xy plane for $z < z_1$ and $z > z_2$, but organize themselves into a vortex sheet for $z_1 < z < z_2$, acting like an extra row of lines in this region. In the region near z_1 and z_2, clearly $\partial_z n_d \neq 0$, corresponding to a nonvanishing value of $\epsilon_{ij}\alpha_{ij}^{\perp}$. Under a constant stress $\sigma_{xz}^{\rm ext}$ from a uniform tilt applied to the system, the Peach-Köhler force on the loop consists again of two forces of equal magnitude applied on the sections running along y and directed along $\pm x$, as there is no force on the sections of the loop running along z. Under the action of this couple, the loop rotates out of its plane. While this motion occurs in the glide plane for each section of the loop, it requires "diffusion" of vacancies and interstitials according to Eq. 4.9.

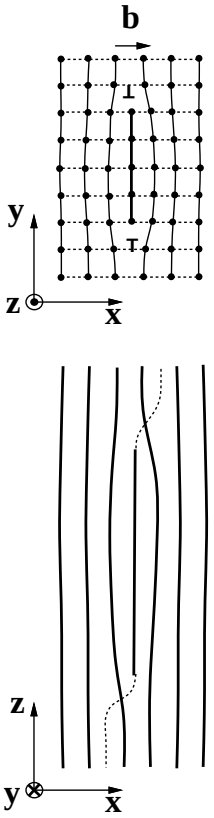

Fig.7.An edge dislocation loop described by a nonvanishing $\alpha_{ij}^{\perp}\epsilon_{ij}$, allowed *only* in the presence of vacancies and interstitials. The bottom figure showing a side view of the loop emphasizes the equivalence between vacancy/interstitial defects and a nonvanishing $\alpha_{ij}^{\perp}\epsilon_{ij}$. The loop can be thought of as arising from an insertion of a row of "finite-length vortices", which correspond to a wandering of interstitial defects.

The addition of dislocations also removes the nonanalyticity of the transverse part of the tilt-tilt correlation function, present in both the defect-free vortex lattice and the vortex supersolid. In fact we obtain

$$T_T(q_\perp, q_z = 0) = n_0^2 k_B T \frac{K + c_{44} + 2(E_s + E_s')q_\perp^2 - 2\gamma'}{Kc_{44} + 2K(E_s + E_s')q_\perp^2 - \gamma'^2}. \tag{4.34}$$

and

$$\begin{aligned} \langle W^2 \rangle &= \lim_{q_\perp \to 0} T_T(q_\perp, q_z = 0) \\ &= \frac{n_0^2 k_B T}{c_{44}^R}, \end{aligned} \tag{4.35}$$

with c_{44}^R given by Eq. 4.25. As indicated in Eq. 2.23, $\lim_{q_\perp \to 0} T_T(q_\perp, q_z = 0)$ determines the winding number $\langle W^2 \rangle$ and the corresponding superfluid density n_s of the equivalent boson system, $\langle W^2 \rangle = \hbar n_s/m$. The analyticity of the transverse tilt-tilt correlator at long wavelength indicates that $n_s = n_0$, i.e., the bosons are in the superfluid state. Conversely, this corresponds to an entangled flux-line array, with no longitudinal superconductivity.

For comparison, in the model of a *constrained* hexatic line liquid, studied by Marchetti and Nelson,[16] where the absence of vacancy/interstitial defects prevents dislocation loops from climbing out of the $(\mathbf{b}, \hat{\mathbf{z}})$ plane, one obtains

$$T_T^{\rm MN}(q_\perp, q_z = 0) = \frac{n_0^2 k_B T}{c_{44} + 2(E_s + E_s')q_\perp^2}, \tag{4.36}$$

and

$$\lim_{q_\perp \to 0} T_T^{\rm MN}(q_\perp, q_z = 0) = \frac{n_0^2 k_B T}{c_{44}}. \qquad (4.37)$$

We find that independent of whether or not vacancy and interstitial defects are included in the description of the hexatic vortex liquid, the transverse tilt-tilt correlator is *analytic* and $\lim_{q_\perp \to 0} T_T(q_\perp, q_z = 0)$ is finite, indicating that both systems are entangled. Vacancies and interstitials do, however, decrease the tilt modulus, further enhancing the entanglement of the vortex array. Although vacancy and interstitial defects must be incorporated in a consistent description of a flux-line hexatic, they do not change the qualitative properties of the hexatic liquid, which even in their presence maintains a vanishing long-wavelength shear modulus and does not exhibit longitudinal superconductivity.

To further characterize orientationally ordered liquid it is useful to define a characteristic length scale $\xi_\perp$, that determines the typical transverse size of a disentangled flux-line bundle. This is a region of the flux array where the lines remain locally disentangled in the limit of infinite sample thickness along the field (z) direction. In the absence of vacancies and interstitials, Eq. (4.36) gives $\xi_\perp^{\rm MN} \sim \sqrt{2(E_s + E_s')/c_{44}}$. Using $E_s \sim E_s' \sim \sqrt{c_{44} c_{66}} b^2$, we find $\xi_\perp^{\rm MN} \sim a_0 (c_{66}/c_{44})^{1/4}$, with $a_0 = \sqrt{1/n_0}$ the mean intervortex separation. In flux-line arrays we typically have $c_{66} << c_{44}$ and the flux-line hexatic is entangled over all macroscopic scales.

The coupling of dislocations to vacancy and interstitial defects renormalizes this entangling length $\xi_\perp$, as can be seen from Eq.4.34, which for small $q_\perp$ is given by

$$T_T(q_\perp, 0) \approx \frac{n_0^2 k_B T}{c_{44}^R} \Big[1 - q_\perp^2 \xi_\perp^2 \Big], \qquad (4.38)$$

with

$$\xi_\perp = \sqrt{\frac{c_{44}^R}{2(E_s + E_s')}} \frac{|K - \gamma'|}{|c_{44} + K - 2\gamma'|}. \qquad (4.39)$$

It is easy to see that for all physical parameter values, $\xi_\perp < \xi_\perp^{\rm MN}$. Not surprisingly, we find that vacancies and interstitials therefore decrease the typical size of a disentangled flux bundle.

Finally, we have also studied the effects of vacancy and interstitial defects on the properties of the orientationally ordered hexatic liquid. Although the finite wavevector behavior is considerably modified, we find that at long wavelength the effective hexatic stiffness is still given by the expression obtained in Ref. 16. This result is consistent with the lack of long-scale orientational order and therefore a vanishing orientational stiffness in the isotropic line-liquid of vacancies and interstitials.

V. CONCLUSIONS

In this paper we have studied the effects of vacancy and interstitial line defects in the supersolid and the liquid phases of flux-line arrays in the mixed state of type-II superconductors.

The transition from a fully ordered Abrikosov crystal phase into the vortex supersolid phase takes place at a critical temperature or magnetic flux density, at which vacancy and interstitial defects proliferate, providing a mechanism for vortex entanglement and yielding finite resistivity. In order to study the long wavelength elastic properties of the supersolid phase, we modeled the supersolid as a lattice with an equilibrium concentration of unbound vacancy and interstitial defect lines and computed the renormalization of the elastic constants due fluctuations in the density and orientations of these defects. As expected, at long wavelengths, we find that vacancy and interstitial density fluctuations do *not* renormalize the shear modulus, confirming the finiteness of the supersolid shear modulus, which distinguishes it from the vortex liquid. In contrast, these defect fluctuations yield a finite downward renormalization of both the compressional and tilt moduli. The renormalization of the tilt modulus stems from the fact that the liquid of vacancy and interstitial defects promotes flux-line wandering. We explicitly demonstrate that this defect-based vortex line delocalization mechanism spoils the Meissner response to a shear tilt perturbation, characteristic of the defect-free vortex lattice. In other words, the vortex supersolid does not exhibit longitudinal superconductivity and, in this respect, similarly to the vortex liquid, is always entangled.

It is clear that the vortex liquid phase, where unbound dislocation loops have proliferated, is also characterized by a finite density of vacancy and interstitials, which *must*, therefore, be included for a consistent description of such a resistive phase. A model of the vortex-line liquid as a solid with an equilibrium concentration of unbound dislocation loops, but no vacancies and interstitials, was previously studied by Marchetti and Nelson[16]. As a consequence of no-vacancy/interstitial constraint implicit in their model, only planar loops, that cannot climb out of their glide plane, were included. We have generalized this model by allowing for a gas of vacancy and interstitial line defects, coupled to the dislocation loop gas and the elastic (phonon) degrees of freedom, to be present in the orientationally ordered vortex liquid. We explicitly demonstrated that a finite concentration of these vacancy and interstitial defects allows the dislocation loops to climb out of their glide plane by emitting and absorbing vacancies and interstitials, and allows for new types of edge dislocations (otherwise forbidden), thereby significantly increasing the entropy of topological defects characterizing the vortex liquid. This physical result is mathematically summarized by Eq.4.9, in which non-planar dislocation loops and horizontal edge dislocations, with Burger's vector in the xy-plane, act as sources for vacancy and interstitial line defects. This resulting climb-like motion provides a mechanism for the relaxation of an externally applied tilt, not present in the model of Ref. 16. We

find, however, that at long wavelengths there is *no independent* renormalization of the tilt and compressional moduli by dislocations, other than that already induced in the supersolid by fluctuations in the density and orientation of vacancy and interstitial defects. This result is somewhat puzzling and may be a consequence of the Debye-Huckel approximation used to here. We are currently investigating the extension of the model presented here beyond the (quadratic) Debye-Huckel treatment of defects in order to answer this question. The coupling of dislocations to vacancy and interstitial defects does, however, affect the response to a shear tilt perturbation that probes longitudinal superconductivity. While both, the vortex supersolid and the vortex liquid fail to exhibit longitudinal superconductivity, and are therefore always entangled, in the supersolid it is only the response of the vacancy and interstitial defects (which form only a small fraction of the total vortex-flux density) that spoils the Meissner effect, as

$$\lim_{q_\perp \to 0} \chi_T^{ss}(q_\perp, q_z = 0) = -\frac{1}{4\pi}\Big(1 - \frac{B^2}{4\pi K}\Big), \qquad (5.1)$$

where K is the tilt modulus of the vacancy-interstitial defect gas. The transverse susceptibility χ_T^{ss}, while larger than $-1/4\pi$– the value required for a perfect Meissner response – remains negative (diamagnetic) and finite. We expect therefore still an appreciable screening of longitudinal currents, running along the applied field direction. In contrast, for the orientationally ordered hexatic vortex liquid (where dislocations loops also unbind), we find

$$\lim_{q_\perp \to 0} \chi_T^{hex}(q_\perp, q_z = 0) = -\frac{1}{4\pi}\Big(1 - \frac{B^2}{4\pi c_{44}^R}\Big), \qquad (5.2)$$

where c_{44}^R is the significantly reduced vortex liquid tilt modulus, given by Eq.4.25. At all, but very low vortex densities $c_{44}^R \approx B^2/4\pi$ and the diamagnetic susceptibility is therefore vanishingly small. Hence, as expected, the fully entangled vortex liquid has essentially normal response to a shear tilt perturbation and exhibits no longitudinal superconductivity.

We hope that the results for the properties of the supersolid and hexatic phases, and as well as for the transitions scenarios from and into them, presented here, will serve as a useful guide for identifying these exotic phases in experiments[24] and simulations[32] of vortex systems. It is also likely that the equilibrium analytical description developed here will be useful for incorporating defects into the current elastic theories of *driven* vortex lattices[44,45], as well as for interpreting and characterizing the results of experiments[46] and numerical simulations[47,48] on these rich nonequilibrium systems.

VI. ACKNOWLEDGMENTS

We both thank The Institute for Theoretical Physics at the University of California Santa Barbara, and the organizers of the Vortex Workshop held there, where this work was initiated, for their hospitality and financial support under NSF Grant No. PHY94-07194. We have benefited from conversations with David Nelson, Daniel Fisher, Erwin Frey and John Toner. MCM was supported by the National Science Foundation at Syracuse through Grants DMR-9730678 and DMR-9805818. LR was financially supported by the National Science Foundation CAREER award, through Grant # DMR-9625111, and by the A.P. Sloan and the David and Lucile Packard Foundations.

VII. APPENDIX A: DETAILS OF COUPLING CONSTANTS APPEARING IN THE SUPERSOLID MODEL

In this appendix we study the phenomenological couplings that appear in our model of a supersolid, defined by the effective free energy F_{ss}, Eq.3.12. Our goal is to determine the range of values that these parameters can assume in a physically realistic model of a supersolid. In Sec.III B we found that the effective supersolid moduli c_{11}^R and c_{44}^R, Eqs.3.23,3.24 vanish at intermediate values of the couplings γ and γ', suggesting a vortex density instability within the supersolid phase. The purpose of this appendix is to show that such an instability is only apparent and arises from our definition of parameters.

As we have seen in Sec.III A, the supersolid effective free energy consists of the elastic lattice part, $F_{\rm latt}$, the vacancy-interstitial defect part, $F_{\rm d}$, and a coupling between the elastic and defect degrees of freedom, $F_{\rm int}$, given in Eq.3.9. The form of $F_{\rm int}$ was dictated by symmetry, with γ and γ' unknown phenomenological parameters. We argue here, however, that in a more realistic model of a supersolid, the coupling between elastic degrees of freedom and defects arises from fluctuations in the magnetic induction, $\delta\mathbf{B}$, and therefore should be written as an expansion in powers of $\delta\mathbf{B}$. To lowest (quadratic) order, such energetic contribution, when expressed in terms of vortex line density fluctuations δn and $\mathbf{t}$, lead to $\tilde{F}_{\rm int}$ given by

$$\tilde{F}_{\rm int} = \frac{1}{2n_0^2}\int d\mathbf{r}\Big[\alpha(\delta n)^2 + \alpha'(\mathbf{t})^2\Big]\,. \qquad (7.1)$$

Inserting the expressions for δn and $\mathbf{t}$ given in Eqs.3.6 and 3.7 in $\tilde{F}_{\rm int}$, expanding the resulting expression and combining it with $F_{\rm latt}$ and $F_{\rm d}$, we find $\tilde{F}_{\rm ss} = F_{\rm latt} + F_{\rm d} + \tilde{F}_{\rm int}$

$$\tilde{F}_{\rm ss} = \frac{1}{2}\int d\mathbf{r}\Big[2\tilde{c}_{66}u_{ij}^2 + (\tilde{c}_{11} - 2\tilde{c}_{66})u_{kk}^2 + \tilde{c}_{44}(\partial_z\mathbf{u})^2 + \frac{1}{\tilde{\chi}n_0^2}(\delta n_d)^2 + \frac{\tilde{K}}{n_0^2}(\mathbf{t}_d)^2 + \frac{2\tilde{\gamma}}{n_0}\delta n_d \boldsymbol{\nabla}\cdot\mathbf{u} + \frac{2\tilde{\gamma}'}{n_0}\mathbf{t}_d\cdot\partial_z\mathbf{u}\Big]\,. \qquad (7.2)$$

Clearly Eq. 7.2 has the same functional form as $F_{\rm ss}$ studied in the main text. The coupling constants, however, are given by

$$\tilde{c}_{11} = c_{11} + \alpha \,, \tag{7.3a}$$
$$\tilde{c}_{66} = c_{66} \,, \tag{7.3b}$$
$$\tilde{c}_{44} = c_{44} + \alpha' \,, \tag{7.3c}$$
$$\tilde{\chi}^{-1} = \chi^{-1} + \alpha \,, \tag{7.3d}$$
$$\tilde{K} = K + \alpha' \,, \tag{7.3e}$$
$$\tilde{\gamma} = -\alpha \,, \tag{7.3f}$$
$$\tilde{\gamma}' = \alpha' \,. \tag{7.3g}$$

and they all depend on the two independent parameters α and α', which are always positive.

We can now reexpress the renormalized supersolid moduli c_{11}^R and c_{44}^R, given by Eqs.3.23 and 3.24, respectively, in terms of the couplings of the model defined here, with the result

$$c_{11}^R = \frac{c_{11}\chi^{-1} + (c_{11} + \chi^{-1})\alpha}{c_{11} + \chi^{-1}} \,, \tag{7.4a}$$
$$c_{44}^R = \frac{c_{44}K + (c_{44} + K)\alpha'}{c_{44} + K} \,, \tag{7.4b}$$

which clearly do not vanish (or diverge) for any positive values of α and α'. Hence the instability found in Sec.III B was spurious, an artifact of expressing our results in terms of γ and γ' and allowing these coupling constants to access values that are unphysical in a generic model of a supersolid.

VIII. APPENDIX B: THE DEFECT FREE ENERGY

Here we give the expressions for the various kernels contained in the defect free energy of Eq.4.23. The nonlocal kernel $\tilde{R}_{\alpha i,\beta j}$ is given by

$$\tilde{R}_{\alpha i,\beta j}(\mathbf{q}) = \frac{1}{q^2} B_{\alpha i,\beta j}(\mathbf{q}) + \Delta_{\alpha i,\beta j}(\mathbf{q}) + E_{\alpha i,\beta j}, \tag{8.1}$$

where

$$B_{\alpha i,\beta j}(\mathbf{q}) = \Big[C_{\alpha i\beta j} - C_{\alpha i\gamma k} q_\gamma (A^{-1})_{kl} q_\eta C_{\eta l\beta j} \Big] \epsilon_{\alpha\lambda\mu} \hat{q}_\lambda \epsilon_{\beta\xi\nu} \hat{q}_\xi, \tag{8.2}$$

describes the long-range interaction between dislocation loops in the absence of vacancy and interstitial defects, while

$$\Delta_{\alpha i,\nu j}(\mathbf{q}) = \frac{1}{q_\perp^2} \Big(K - \frac{\gamma'^2 q_z^2}{\Gamma_L} \Big) \epsilon_{z\alpha i} \epsilon_{z\beta j} - \frac{\gamma' \hat{q}_{\perp k}}{q^2} \big[\epsilon_{zk\alpha} \hat{q}_{\perp i} \epsilon_{z\beta j} + \epsilon_{zk\beta} \hat{q}_{\perp j} \epsilon_{z\alpha i} \big] \tag{8.3}$$
$$+ \frac{\gamma' q_z q_\mu q_\gamma \hat{q}_{\perp k}}{q^2 q_\perp \Gamma_L} \big[C_{\mu k\nu i} \epsilon_{\nu\gamma\alpha} \epsilon_{z\beta j} + C_{\mu k\nu j} \epsilon_{\nu\gamma\beta} \epsilon_{z\alpha i} \big]. \tag{8.4}$$

is the part of such interaction mediated by vacancy and interstitial defects. The matrix $E_{\alpha i,\beta j}$ describes the dislocation core energy and is given by

$$E_{\alpha i,\beta j} = 2E_e \delta_{\alpha z}\delta_{\beta z}\delta_{ij} + 2E_s \delta_{\alpha i}\delta_{\beta j} + 2E_s' \delta_{\alpha\beta}(1 - \delta_{\alpha z}\delta_{\beta z})\delta_{ij} + 2E_e' \epsilon_{z\alpha i}\epsilon_{z\beta j}. \tag{8.5}$$

The effective interaction between the vacancy and interstitial defects is described by the two scalar kernels

$$A(\mathbf{q}) = \frac{1}{n_0^2} \Big[\chi^{-1} + K \frac{q_z^2}{q_\perp^2} - \big(\gamma - \gamma' q_z^2/q_\perp^2 \big)^2 \frac{q_\perp^2}{\Gamma_L} \Big], \tag{8.6}$$

and

$$C(\mathbf{q}) = \frac{1}{n_0^2} \Big[K - \frac{\gamma'^2 q_z^2}{\Gamma_T} \Big]. \tag{8.7}$$

Finally, the tensors $D_{\alpha i}$ and $G_{\alpha i}$ describe the coupling between the dislocation loop gas and the liquid of vacancy-interstitial defect lines, and are given by

$$D_{\alpha i}(\mathbf{q}) = \frac{1}{n_0 q} \Big\{ \big[\gamma \delta_{\beta i} - \gamma' \delta_{\beta z} \hat{q}_{\perp i} q_z/q_\perp \big] - \frac{q_\perp}{\Gamma_L} \big(\gamma - \gamma' q_z^2/q_\perp^2 \big) q_\mu \hat{q}_{\perp i} C_{\mu j\beta i} \Big\} \epsilon_{\beta\gamma\alpha} \hat{q}_\gamma - \frac{q_z}{n_0} \Big[\frac{K}{q_\perp^2} + \frac{\gamma'}{\Gamma_L} \big(\gamma - \gamma' q_z^2/q_\perp^2 \big) \Big] \epsilon_{z\alpha i}, \tag{8.8}$$

$$G_{\alpha i}(\mathbf{q}) = \frac{\gamma'}{n_0 q} \Big[\gamma \delta_{\beta z} \hat{C}_i - \frac{q_z}{\Gamma_T} q_\mu \hat{C}_j C_{\mu j\beta i} \Big] \epsilon_{\beta\gamma\alpha} \hat{q}_\gamma, \tag{8.9}$$

with $\hat{C}_i = \epsilon_{ij} \hat{q}_{\perp j}$ and $\hat{q}_\xi = q_\xi/q$,

[1] D. Huse and L. Radzihovsky, in Proceedings of 1993 Altenberg Summer School, *Fundamental Problems in Statistical Mechanics VIII*, edited by H. van Beijeren and M. H. Ernst (Elsevier, Netherlands).
[2] G. Blatter, M.V. Feigel'man, V.B. Geshkenbein, A.I. Larkin, and V.M. Vinokur, Rev. Mod. Phys. **66**, 1125 (1994).
[3] E. H. Brandt, Rep. Prog. Phys. **58**, 1465 (1995).
[4] D.R. Nelson, Phys. Rev. Lett. **60**, 1973 (1988); D.R. Nelson and S. Seung, Phys. Rev. B **39**, 9153 (1989).
[5] As first pointed out in Ref. 4, one also expects a vortex liquid state to exist just above the $H_{c1}(T)$ curve, in very clean superconductor samples.
[6] M. P. A. Fisher, Phys. Rev. Lett. **62**, 1415 (1989); D. S. Fisher, M. P. A. Fisher, and D. A. Huse, Phys. Rev. B **43**, 130 (1991).
[7] A. Larkin, Sov. Phys. JETP **31**, 784 (1970); A.I. Larkin and Y.N. Ovchinnikov, Sov. Phys. JETP **38**, 854 (1974).
[8] T. Giamarchi and Le Doussal, Phys. Rev. Lett. **72**, 1530 (1994); M.J.P. Gingras and D.A. Huse, Phys. Rev. B **53**, 15183; D. S. Fisher, Phys. Rev. Lett. **78**, 1964 (1997). In ultra-clean superconductors, the distinction between the conventional ordered Abrikosov lattice and the Bragg glass appears, however, only beyond a very large Larkin scale.[7] Analogous topologically ordered, but elastically disordered phases also appear in other randomly pinned periodic systems, such as for example smectic liquid crystals confined in aerogel: L. Radzihovsky and J. Toner, Phys. Rev. Lett. **79**, 4214 (1997); B. Jacobsen, K. Saunders, L. Radzihovsky and J. Toner, unpublished.
[9] P.L. Gammel, L.F. Scheemeyer, J.V. Waszczak, and D.J. Bishop, Phys. Rev. Lett. **61**, 1666 (1988).
[10] R.H. Koch et al., Phys. Rev. Lett. **63**, 1511 (1989).
[11] E. Zeldov et. al, Nature **382**, 791 (1996).
[12] Although a clean vortex crystal appears to melt via a first order transition, as first observed in Ref. 11, a fluctuation-driven *continuous* melting transition is theoretically possible, as demonstrated for model systems in Ref. 13.
[13] L. Radzihovsky, Phys. Rev. Lett. **74**, 4722 (1995); L. Balents and L. Radzihovsky, Phys. Rev. Lett. **76**, 3416 (1996). S.A. Ktitorov, B.N.Shalaev, and L. Jastrabik, Phys. Rev. B **49**, 15248 (1994).
[14] J.M. Kosterlitz and D.J. Thouless, J. Phys. C**6**, 1181 (1973); B. I. Halperin and D. R. Nelson, Phys. Rev. Lett. **41**, 121 (1978); D. R. Nelson and B. I. Halperin, Phys. Rev. B **19**, 2457 (1979); A. P. Young, Phys. Rev. B **19**, 1855 (1979).
[15] D.S. Fisher, Phys. Rev. B **22**, 1190 (1980).
[16] M.C. Marchetti and D.R. Nelson, Phys. Rev. B **41**, 1910 (1990).
[17] D.R. Nelson and J. Toner, Phys. Rev. B **24**, 363 (1981).
[18] P. C. Martin, O. Parodi, and P.S. Pershan, Phys. Rev. A **6**, 2401 (1972).
[19] M. P. A. Fisher and D. H. Lee, Phys. Rev. B **39**, 2756 (1989).
[20] E. Frey, D.R. Nelson and D.S. Fisher, Phys. Rev. B **49**, 9723 (1994).
[21] L.I. Glazman and A.E. Koshelev, Phys. Rev. B **43**, 2835 (1991).
[22] E. Frey and L. Balents, Phys. Rev. B **55**, 1050 (1997).
[23] D.T. Fuchs, E. Zeldov, T. Tamegai, S. Ooi, M. Rappaport, and H. Shtrikman, Phys. Rev. Lett. **80**, 4971 (1998).
[24] E.M. Forgan *et al.*, Czech. J. Phys. **46**, 1571 (1996).
[25] Since in type I melting two order parameters (vacancy-interstitial density and dislocation density) with unrelated symmetry order simultaneously, we expect type I melting to be 1st order. In contrast, type II melting can be continuous, consisting of 3 intermediate transitions: solid-to-supersolid, supersolid-to-hexatic, and hexatic-to-(isotropic) liquid (see Ref. 13).
[26] In a vortex liquid dislocations are, by definition, unbound. Furthermore, a pair of dislocations forms a vacancy or an interstitial defect. We expect therefore that there will always be a finite density of vacancy and interstitial defects in the liquid phase.
[27] The relation to the Lamé coefficients μ and λ, commonly used in the study of elasticity of solids is: $c_{66} = \mu$ and $c_{11} = 2\mu + \lambda$.
[28] E.H. Brandt and U. Essman, Phys. Status Solidi B **144**, 13 (1987).
[29] D.S. Fisher, in *Phenomenology and Applications of High-Temperature Superconductors*, K.S. Bedell et al., eds. (Addison-Wesley, 1992), p. 287.
[30] D.R. Nelson and P. Le Doussal, Phys. Rev. B **42**, 10113 (1990).
[31] More generally the relationship between the hydrodynamic fields and the local induction is nonlocal and can be obtained by solving the anisotropic London equation, as shown for instance in Ref. 30.
[32] T. Chen and S. Teitel, Phys. Rev. B **55**, 15197 (1997).
[33] D. R. Nelson and V. M. Vinokur, Phys. Rev. Lett. **68**, 2398 (1992); Phys. Rev. B. **48**, 13060 (1993).
[34] E.L. Pollock and D.M. Ceperley, Phys. Rev. B**36**, 8343 (1987).
[35] P. Benetatos and M.C. Marchetti, to appear in Phys. Rev. B (cond-mat/9808270).
[36] L. Radzihovsky and E. Frey, Phys. Rev. B, **48**, 10357 (1993).
[37] M.C. Marchetti and D.R. Nelson, Physica C **174**, 40 (1991).
[38] H.M. Carruzzo and C.C. Yu, Phil. Mag. B **77**, 1001 (1998).
[39] A. Zippelius, B.I. Halperin and D.R. Nelson, Phys. Rev. B **22**, 2514 (1980).
[40] We note in passing that from this expression we see that the stability of a defect-free crystal is determined by the two conditions: (i) $c_{66} > 0$ and (ii) $c_{11} > c_{66}$ (or equivalently in Landau and Lifshitz notation $\mu > 0$ and $\mu + \lambda > 0$), derived from the requirement of a finite zero mode response to a *uniform* stress. This condition is different and more stringent than that imposed by the requirement of a finite response of the finite wavevector bulk modes ($u_T(\mathbf{q})$ and $u_L(\mathbf{q})$), obtained from the propagator of F_{el} Eq.3.12, which gives: (i) $c_{66} > 0$ and (ii) $c_{11} > 0$.
[41] F.R.N. Nabarro and A.T. Quintanilha, in *Dislocations in Solids*, edited by F.R.N. Nabarro (North-Holland, Amster-

dam, 1980), Vol. 5.
[42] E.H. Brandt, Phys. Rev. B **34**, 6514 (1986); Jpn. J. Appl. Phys. **26**, 1515 (1987).
[43] These renormalized moduli can also be obtained by simply integrating out the *defect* degrees of freedom δn_d and t_d^T inside the partition function, and identifying the corresponding effective elastic moduli in the remaining effective elastic free energy functional.
[44] S. Scheidl and V.M. Vinokur, unplublished (cond-mat/9702014).
[45] L. Balents, M.C. Marchetti, and L. Radzihovsky, Phys. Rev. B **57**, 7705 (1998).
[46] E.Y. Andrei, G. Deville, D.C. Glattli, F.I.B. Williams, E. Paris, and B. Etienne, Phys. Rev. Lett. **60**, 2765 (1988).
[47] K. Moon, R. T. Scalettar, and G. Zimányi, Phys. Rev. Lett. **77**, 2778 (1996).
[48] C.J. Olson, C. Reichhardt, and F. Nori, Phys. Rev. Lett. **80**, 2197 (1998), ibid. **81**, 3757 (1998).